molecular pharmaceutics

Article

pubs.acs.org/molecularpharmaceutics

Design, Synthesis, and Evaluation of Linker-Duocarmycin Payloads: Toward Selection of HER2-Targeting Antibody–Drug Conjugate SYD985

Ronald C. Elgersma,[†] Ruud G. E. Coumans,[†] Tijl Huijbregts,[†] Wiro M. P. B. Menge,[†] John A. F. Joosten,[†] Henri J. Spijker,[†] Franciscus M. H. de Groot,[†] Miranda M. C. van der Lee,[‡] Ruud Ubink,[‡] Diels J. van den Dobbelsteen,[‡] David F. Egging,[‡] Wim H. A. Dokter,[‡] Gijs F. M. Verheijden,[§] Jacques M. Lemmens,[§] C. Marco Timmers,[§] and Patrick H. Beusker*[,†]

Departments of [†]Medicinal & Protein Chemistry, [‡]Preclinical, and [§]New Molecular Entities, Synthon Biopharmaceuticals BV, Microweg 22, 6545 CM Nijmegen, The Netherlands

Supporting Information

ABSTRACT: Antibody–drug conjugates (ADCs) that are currently on the market or in clinical trials are predominantly based on two drug classes: auristatins and maytansinoids. Both are tubulin binders and block the cell in its progression through mitosis. We set out to develop a new class of linker-drugs based on duocarmycins, potent DNA-alkylating agents that are composed of a DNA-alkylating and a DNA-binding moiety and that bind into the minor groove of DNA. Linker-drugs were evaluated as ADCs by conjugation to the anti-HER2 antibody trastuzumab via reduced interchain disulfides. Duocarmycin **3b**, bearing an imidazo[1,2-*a*]pyridine-based DNA-binding unit, was selected as the drug moiety, notably because of its rapid degradation in plasma. The drug was incorporated into the linker-drugs in its inactive prodrug form, *seco*-duocarmycin **3a**. Linker attachment to the hydroxyl group in the DNA-alkylating moiety was favored over linking to the DNA-binding moiety, as the first approach gave more consistent results for in vitro cytotoxicity and generated ADCs with excellent human plasma stability. Linker-drug **2** was eventually selected based on the properties of the corresponding trastuzumab conjugate, SYD983, which had an average drug-to-antibody ratio (DAR) of about 2. SYD983 showed subnanomolar potencies against multiple human cancer cell lines, was highly efficacious in a BT-474 xenograft model, and had a long half-life in cynomolgus monkeys, in line with high stability in monkey and human plasma. Studies comparing ADCs with a different average DAR showed that a higher average DAR leads to increased efficacy but also to somewhat less favorable physicochemical and toxicological properties. Fractionation of SYD983 with hydrophobic interaction chromatography resulted in SYD985, consisting of about 95% DAR2 and DAR4 species in an approximate 2:1 ratio and having an average DAR of about 2.8. SYD985 combines several favorable properties from the unfractionated ADCs with an improved homogeneity. It was selected for further development and recently entered clinical Phase I evaluation.

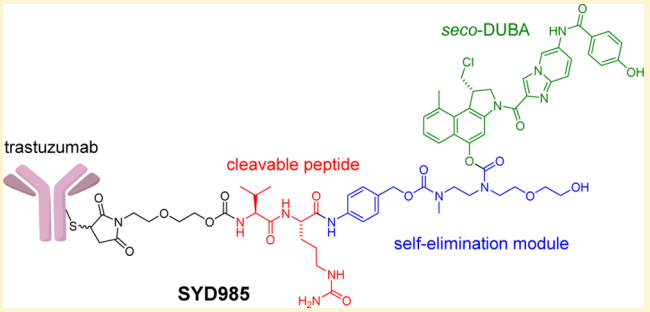

KEYWORDS: *duocarmycin, linker-duocarmycin, antibody–drug conjugate, ADC, structure–activity relationship, drug targeting, design, seco-DUBA, DUBA, SYD983, SYD985, HER2*

INTRODUCTION

Antibody–drug conjugates (ADCs) are more and more considered to be valuable therapeutics for cancer therapy and a still increasing number of companies are actively developing ADCs. The recent approvals of Adcetris (brentuximab vedotin)[1] and Kadcyla (ado-trastuzumab emtansine)[2] for the treatment of CD30- and HER2-positive cancers, respectively, have significantly contributed the excitement to the use of ADC therapeutics for cancer treatment. Over 30 ADCs are currently in clinical trials and more are in preclinical development. Most of these ADCs, including brentuximab vedotin and ado-trastuzumab emtansine, use auristatins or maytansinoids as payloads. Both are tubulin polymerization inhibitors that bind to the vinca domain in tubulin and that cause cell cycle arrest in the G2-M phase, eventually leading to apoptotic cell death. There are only a small number of ADCs in clinical development that contain different drug classes, including calicheamycins, camptothecins, anthracyclines, and pyrroloben-

Special Issue: Antibody-Drug Conjugates

Received: November 24, 2014
Revised: January 21, 2015
Accepted: January 30, 2015
Published: January 30, 2015

DOI: 10.1021/mp500781a
Mol. Pharmaceutics 2015, 12, 1813–1835

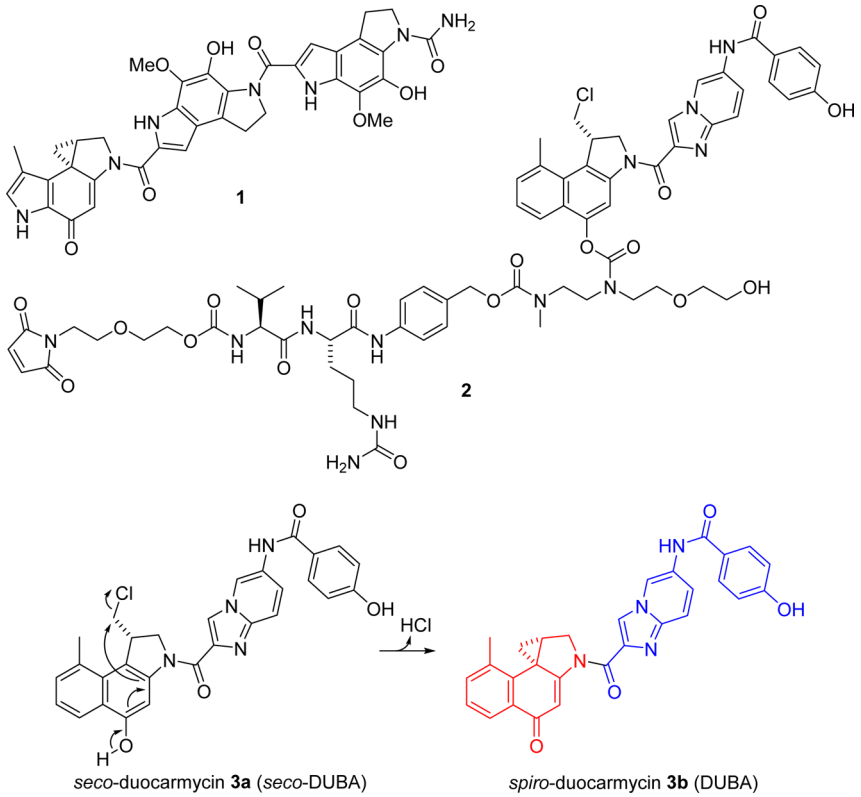

Figure 1. Structures of CC-1065 (**1**) and linker-duocarmycin **2**, and schematic representation of the Winstein spirocyclization of *seco*-duocarmycin **3a** (*seco*-DUBA) to its *spiro* analogue **3b** (DUBA). The DNA-alkylating unit in **3b** is indicated in red, the DNA-binding unit in blue.

zodiazepine dimers,[3] which all target DNA or DNA-related proteins. Other drug classes, such as aminitins,[4] tubulysins,[4] and monofunctional indolinobenzodiazepine dimers,[5] are being explored preclinically and may enter the clinic in the years to come.

Although ADCs generally show an enhanced selectivity toward tumor cells compared to nontargeted chemotherapeutics, still a considerable number of off-target toxicities and side effects are noted in a significant number of patients. This is most likely due to the fact that ADCs, like traditional chemotherapeutics, are dosed at the maximum tolerated dose, and consequently, adverse effects are notable. For brentuximab vedotin, given to patients at a dose level of 2.4 mg/kg every 3 weeks, peripheral sensory neuropathy and neutropenia are commonly observed grade ≥3 adverse events.[6−8] Similarly, thrombocytopenia and neutropenia are frequently observed for ado-trastuzumab emtansine, which is administered at a dose level of 3.6 mg/kg every 3 weeks.[9−12] For these ADCs, as well as for other ADCs based on the same drug classes that are still in clinical development, many of the reported toxicities appear to be identical and target-independent, suggesting that many toxicities are related to (systemic) exposure to the drug.[13]

The first discovered member of the naturally occurring duocarmycins was CC-1065 (**1**, Figure 1), isolated from *Streptomyces* bacteria in the late 1970s.[14] Duocarmycins act by binding to the minor groove of DNA in A-T rich regions and subsequently alkylating adenine residues at the N3 position through the cyclopropyl group in the DNA-alkylating moiety.[15] Although CC-1065 was shown to be very potent in vitro, it demonstrated only moderate in vivo activity[16] and delayed lethality accompanied by irreversible hepatic toxicity[17] in animal models. Many groups have been working on the development of synthetic duocarmycin analogues with the aim to improve the biological profile of this class of compounds.[18−21]

Halogen-containing *seco* derivatives of the duocarmycins are generally believed to require a ring closure to their cyclopropyl-containing *spiro* analogues (Figure 1) to become cytotoxic, although *seco* derivatives that cannot rearrange to their *spiro* counterparts have been shown to have DNA-alkylating capabilities as well, albeit much more attenuated.[22,23] Thus, by trapping the duocarmycin in its *seco* form through conjugation of the crucial hydroxyl group to a promoiety, the duocarmycin drug can be (largely) inactivated until the promoiety is removed and ring closure to the *spiro* form can occur. This concept has, for example, been applied to duocarmycin prodrugs carzelesin and KW-2189, which both progressed into clinical development. Unfortunately, like nonprodrug adozelesin, which was also evaluated in the clinic,[24] both compounds lacked sufficient therapeutic window, related to hematological toxicity, and clinical development was halted.[25,26]

In an effort to develop a class of linker-drugs that would allow for ADCs with an improved therapeutic index and with a mechanism of action distinct from that of ADCs currently on the market or in clinical development, we have explored the duocarmycin class of compounds as ADC drugs. Others[27−30] have also studied this drug class for use in ADCs, but only one duocarmycin-based ADC, MDX-1203[31] (now BMS-936561[32]), was progressed into Phase I clinical trials. However, to the best of our knowledge, no clinical trials were ongoing with this ADC at the time of writing this article.

Here, we describe a new duocarmycin derivative with the favorable in vitro and in vivo properties to use it as an ADC.

DOI: 10.1021/mp500781a
Mol. Pharmaceutics 2015, 12, 1813−1835

Scheme 1. Synthesis of DNA-Alkylating Unit 15[a]

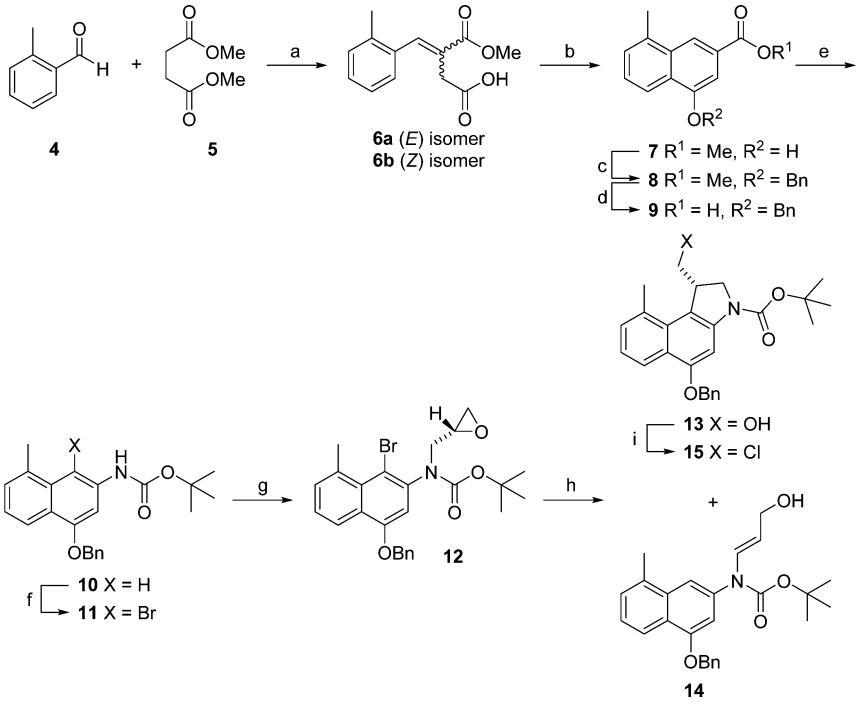

[a]Reagents and conditions: (a) NaOMe, MeOH, 65−80 °C, 1 h; (b) TFAA, THF, reflux, 42% (2 steps); (c) BnCl, DMF, 80 °C; (d) NaOH, water/MeOH/toluene, reflux, 2 h, 82% (2 steps); (e) DPPA, *t*-BuOH, Et_3N, toluene, 85 °C, 3 h, 88%; (f) NBS, THF, −10 °C; (g) (*S*)-glycidyl nosylate, KO*t*-Bu, 10 to 25 °C, 3 h, 82% (2 steps); (h) *n*-BuLi, THF, −25 °C, 1 h, 40% (**13**); (i) (1) MsCl, Et_3N, CH_2Cl_2, 0 °C, 90 min; (2) LiCl, DMF, 80 °C, 90 min, 63% (2 steps).

This duocarmycin was incorporated into novel linker-duocarmycin constructs using linkers optimized to provide a perfect synergy with the drug. ADCs based on these linker-duocarmycins and the anti-HER2 antibody trastuzumab were extensively evaluated, eventually culminating in selection of linker-duocarmycin **2** as the lead linker-drug for our anti-HER2 ADC program and subsequent development of HER2-targeted ADC SYD985, which recently entered clinical development.

RESULTS

Duocarmycins. The hydrophobic nature of duocarmycins conveys a strong binding into the minor groove of DNA, but at the same time, it limits the water solubility of this class of compounds. Furthermore, it was shown by Jeffrey and co-workers[28] to adversely affect physicochemical properties of duocarmycin-based ADCs, as relatively high amounts of high molecular weight (HMW) species were observed when a linker was used that had successfully been employed for other drug classes. By reducing linker hydrophobicity, the amount of HMW species could be lowered. We envisioned that hydrophobicity could potentially also be reduced by introduction of heteroatoms at selected positions within the core ring structure of the duocarmycin itself. An extensive structure−activity relationship study focusing on the effects of structural modifications on CMC and preclinical properties of the duocarmycins and their corresponding ADCs led to identification of the imidazo[1,2-*a*]pyridine series as an interesting class of duocarmycins. Analogue **3a** (*seco*-DUBA, Figure 1) was selected from this class based on its favorable properties.

seco-DUBA was prepared from the corresponding DNA-alkylating and DNA-binding moieties. The DNA-alkylating moiety, which is based on the 1,2,9,9a-tetrahydrocyclopropa[*c*]benzo[*e*]indole-4-one framework,[33,34] was prepared according to the route depicted in Scheme 1.

Starting from *o*-tolualdehyde (**4**) and dimethyl succinate (**5**), a 9:1 mixture of acids **6a** and **6b** was obtained through a Stobbe condensation.[35] Ring closure of the mixture of acids was accomplished with trifluoroacetic anhydride and gave alcohol **7**, which was then protected with benzyl chloride to afford benzyl ether **8**. Ensuing hydrolysis of the methyl ester group in **8** to afford carboxylic acid **9** was followed by a Curtius rearrangement in a mixture of toluene and *tert*-butyl alcohol to provide carbamate **10**. Bromination with *N*-bromosuccinimide to give bromide **11** proceeded smoothly. Besides chromatographic resolution and diastereomeric derivatization, asymmetric synthetic approaches, such as enzymatic desymmetrization reactions,[36] asymmetric hydroboration,[37] and Jacobsen epoxidation,[37] have been used to obtain the alkylating moiety with high enantiomeric excess. We decided to alkylate bromide **11** with (*S*)-glycidyl nosylate[38−40] to be able to introduce the five-membered ring. Alkylation proceeded well in the presence of potassium *tert*-butoxide and gave epoxide **12** in good yield. Ring closure proved unsuccessful with many organometallic reagents, most likely due to steric congestion at the reaction site. The reaction with *n*-butyllithium gave the best results and provided a mixture of desired compound **13** and debrominated, rearranged derivative **14**. The ratio between **13** and **14** was strongly dependent on the reaction conditions that were used. Yields for **13** proved to be highest when tetrahydrofuran was used as the solvent and the reaction temperature was kept between −25 and −20 °C. Under these conditions, **13** and **14** were obtained in an approximate 1:1 ratio. Separation of the two compounds proved difficult, but workup with *p*-toluenesulfonic acid resulted in conversion of **14** to **10**,

DOI: 10.1021/mp500781a
Mol. Pharmaceutics 2015, 12, 1813−1835

Scheme 2. Synthesis of *seco*-DUBA (3a) via DNA-Binding Unit 22 and DNA-Alkylating Unit 15[a]

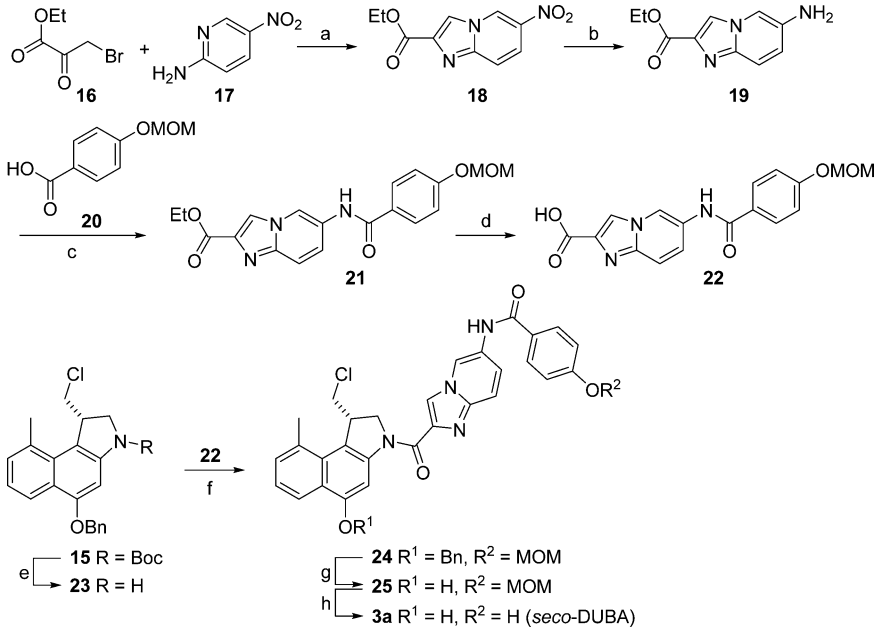

[a]Reagents and conditions: (a) EtOH, 85 °C, 22 h, 89%; (b) HCl, Zn, MeOH, 0 °C, 30 min, 68%; (c) EDC, DMA, 18 h; (d) NaOH, 1,4-dioxane/water, 70 °C, 30 min, 55% (2 steps); (e) HCl, dioxane, 4 h; (f) EDC, DMA, 0 to 20 °C, 18 h, 93% (2 steps); (g) Pd/C, NH_4HCO_2, MeOH/THF, 3 h, 90%; (h) HCl, 1,4-dioxane/water, 1 h, 95%.

which made separation possible. Mesylation of the hydroxyl group in **13** followed by chloride substitution using lithium chloride gave key intermediate **15**.

The DNA-binding moiety of *seco*-DUBA was prepared according to the route depicted in Scheme 2. A Chichibabin cyclization reaction[41] between commercially available ethyl bromopyruvate (**16**) and 5-nitropyridin-2-amine (**17**) was used to obtain nitro compound **18**. Reduction of the nitro group with zinc under acidic conditions gave amine **19**. Next, coupling with methoxymethyl (MOM)-protected 4-hydroxybenzoic acid (**20**), prepared from methyl 4-hydroxybenzoate through reaction with chloromethyl methyl ether followed by ester hydrolysis,[42] gave ethyl ester **21**, which was hydrolyzed with sodium hydroxide in aqueous 1,4-dioxane to provide acid **22**.

seco-DUBA was synthesized from DNA-alkylating unit **15** and DNA-binding moiety **22** by removal of the *tert*-butoxycarbonyl (Boc) protective group from **15** under acidic conditions followed by EDC-mediated coupling of amine **23** to acid **22**. Compound **24** was then fully deprotected in two consecutive steps to afford *seco*-DUBA as its HCl salt.

seco-DUBA was evaluated in three human cancer cell lines, selected based on their HER2 status: breast carcinoma cell line SK-BR-3 (HER2 3+), ovarian carcinoma cell line SK-OV-3 (HER2 2+), and colon carcinoma cell line SW620 (HER2-negative).[43] All cell lines were highly sensitive to *seco*-DUBA with IC_{50} values ranging from 90 to 430 pM (Table 1).

The presence of the second nitrogen atom in the ring structure of the DNA-binding moiety of *seco*-DUBA proved to have a positive effect on logP. *seco*-DUBA and its analogue **26** (Chart 1) were calculated to have logP values of 4.32/4.14 and 4.64/4.68, respectively,[44] indicating a decreased hydrophobicity for *seco*-DUBA with respect to its analogue **26**. Calculated values for *seco*-DUBA were in line with the experimentally determined logD value of 3.7 at pH 7.4, especially if one considers that the DNA-binding moiety in *seco*-DUBA is expected to be partly protonated at physiological pH since the pK_a of the imidazo[1,2-*a*]pyridine group is estimated to be close to 6.[45,46]

Table 1. IC_{50} Values for *seco*-DUBA (3a), DUBA (3b), 27, 28, and DAR 2 ADCs Tmab-29, Tmab-30, SYD981 (Tmab-45), and SYD983 (Tmab-2) in a Panel of Human Cancer Cell Lines Expressing Different Levels of HER2[a]

	IC_{50} (nM)				
compd	SK-BR-3	SK-OV-3	SW620	SW620 + 1% MP	SW620 + 1% HP
seco-DUBA	0.09	0.43	0.09	0.16	0.22
DUBA	0.07				
27	4,933	-	-	-	-
28	>30,000	-	-	-	-
Tmab-**29**	0.19	0.51	±100	0.46	±100
Tmab-**30**	2.01	0.66	>100	2.53	>100
SYD981	0.31	1.20	>100	3.95	>100
SYD983	0.22	0.44	±100	0.93	±100

[a]SK-BR-3 (HER2 3+), SK-OV-3 (HER2 2+), and SW620 (HER2-negative) cells were incubated with compound for 144 h, after which cell viability was assessed. Nontarget-related drug release by 1% mouse plasma (MP) or human plasma (HP) was measured by detection of cell viability of HER2-negative SW620 cells. For ADCs, IC_{50} values are expressed in drug equivalents.

DUBA (**3b**), formed through spontaneous spirocyclization of *seco*-DUBA (Figure 1), was shown to be equally potent and efficacious as *seco*-DUBA in SK-BR-3 cells, which suggests that spirocyclization is not rate-limiting. DUBA was found to be relatively unstable in buffer at physiological pH (data not shown) and in plasma from Balb/c mice, Wistar rats, cynomolgus monkeys, and man when incubated at a concentration of 5 nM. Half-lives were determined to be 5.3, 0.6, 1.6, and 1.0 h in mouse, rat, monkey, and human plasma, respectively. Percentages of DUBA remaining after 180 min of

DOI: 10.1021/mp500781a
Mol. Pharmaceutics 2015, 12, 1813−1835

Chart 1. Structures of *seco*-Duocarmycin 26, DNA-Alkylating Unit 27, DNA-Binding Unit 28, and Linker-Duocarmycins 29, 30, and 45

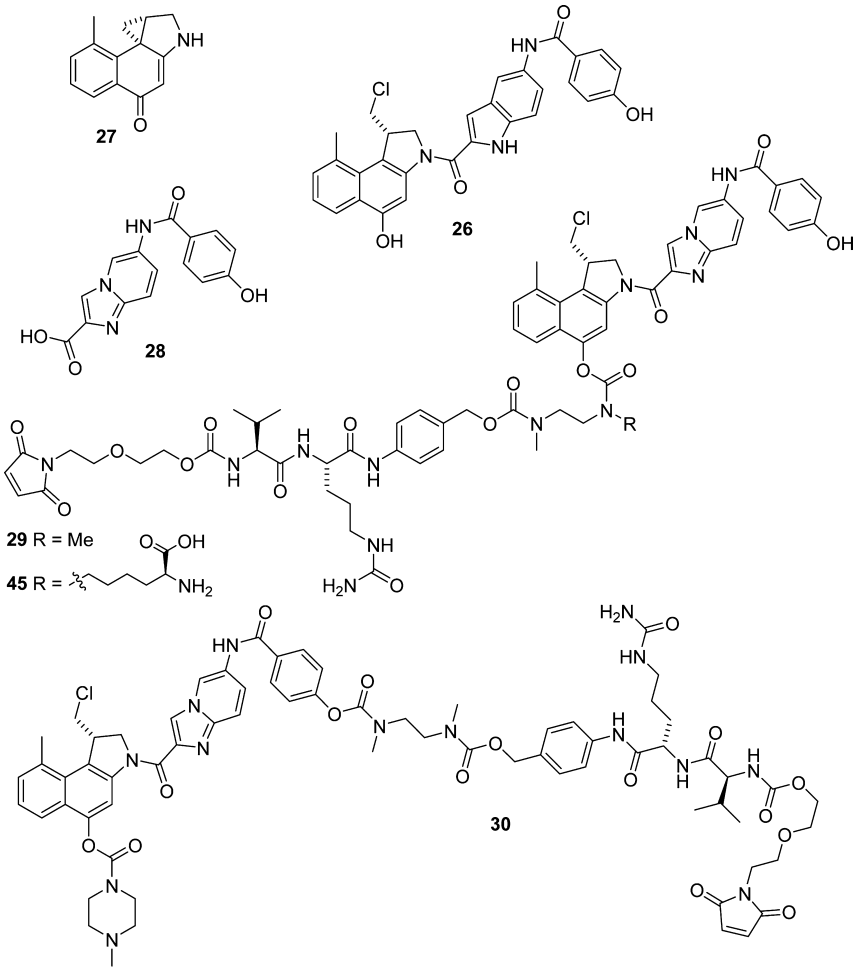

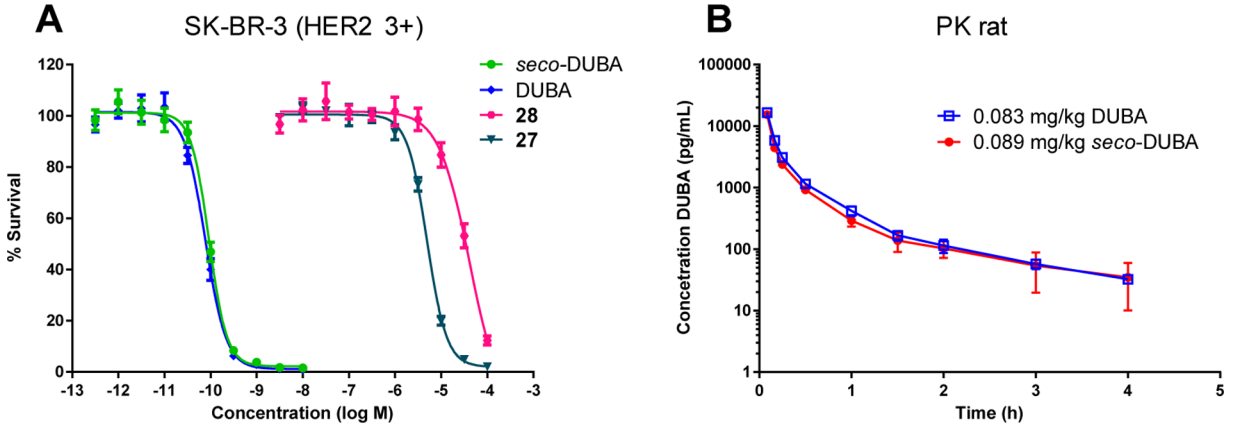

Figure 2. (A) Comparison of the in vitro cytotoxicity of *seco*-DUBA, DUBA, **27**, and **28** against SK-BR-3 cells after 144 h of incubation. (B) Plasma concentration vs time curve for DUBA in Wistar rats after a single intravenous injection of *seco*-DUBA (89 μg/kg) or DUBA (83 μg/kg) (n = 4, ±SEM).

incubation were 68.2% in mouse plasma, 2.6% in rat plasma, 44.5% in monkey plasma, and 27.0% in human plasma. Plasma stability of DUBA was about 3-fold lower than that of the spirocyclized analogue of **26**, indicating that the presence of the additional heteroatom in the DNA-binding moiety had a substantial effect on plasma stability. A main degradation pathway of DUBA was shown to comprise hydrolysis of the amide bond between the DNA-alkylating moiety and DNA-binding moiety, resulting in formation of DNA-alkylating unit **27** and DNA-binding unit **28** (Chart 1).

Both **27** and **28** showed over 50,000-fold reduced potency against SK-BR-3 cells (Figure 2A, Table 1), indicating that hydrolysis is an important detoxification route of the drug. When ring closure of *seco*-DUBA to its *spiro* analogue was

DOI: 10.1021/mp500781a
Mol. Pharmaceutics 2015, 12, 1813−1835

Scheme 3. Synthesis of Linker-Drug 29[a]

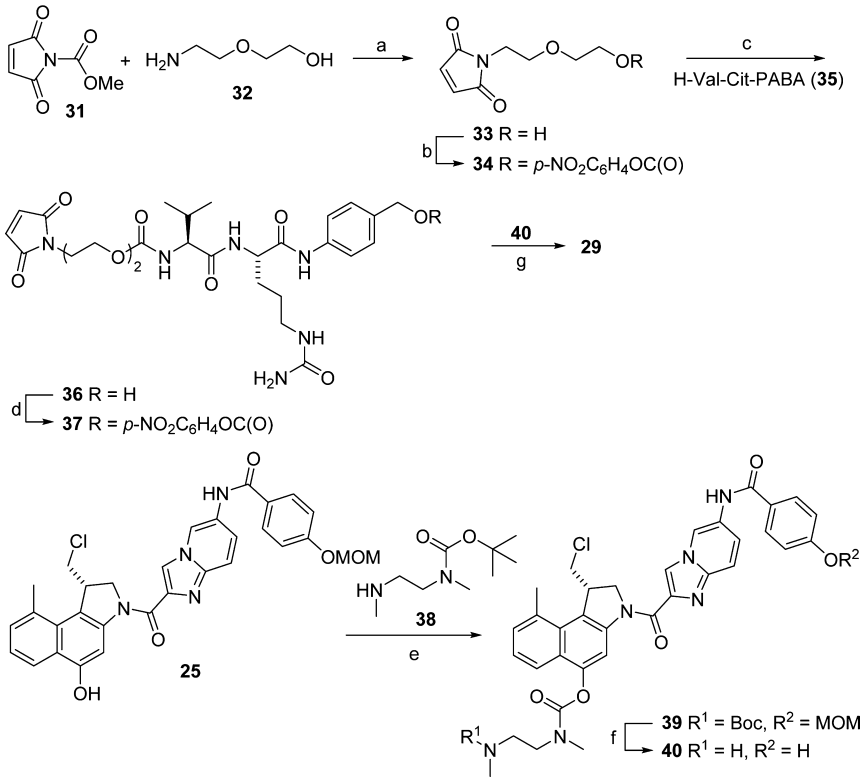

[a]Reagents and conditions: (a) $NaHCO_3$, water, 0 °C to room temperature, 50 min, 73%; (b) 4-nitrophenyl chloroformate, Et_3N, CH_2Cl_2, 2.5 h, 95%; (c) **35**, *i*-Pr_2NEt, DMF, 0 °C; (d) bis(4-nitrophenyl) carbonate, *i*-Pr_2NEt, DMF, 0 °C, 2 h, 77% (2 steps); (e) 4-nitrophenyl chloroformate, Et_3N, THF, 0 °C, 1.5 h; then **38**, 1 h, 93%; (f) TFA, CH_2Cl_2, 0 °C, 1 h; (g) Et_3N, DMF, 0 °C to room temperature, 2 h, 49% (2 steps).

prevented by coupling of a linker to the hydroxyl group in the alkylating moiety, hydrolysis was not detected, suggesting that the *spiro* form is required for hydrolysis to occur.

Although the low plasma stability of DUBA may seem deleterious for biological activity, we believed that it could positively affect the profile of ADCs based on *seco*-DUBA, as rapid degradation of DUBA in plasma would translate to low systemic exposure to the drug and consequently a lower probability for off-target toxicity.

To corroborate the low stability of DUBA in vivo, a pharmacokinetic study with *seco*-DUBA and DUBA was conducted in Wistar rats. This study indicated once more that *seco*-DUBA is likely converted to DUBA almost instantaneously, as DUBA pharmacokinetics were very similar after administration of DUBA and *seco*-DUBA at an equimolar dose (Figure 2B). No *seco*-DUBA could be detected in plasma, and DUBA was rapidly cleared from the systemic circulation, showing a very high clearance of 17 L/(h·kg) and a terminal half-life of 1.1 h. The instability observed in plasma in vitro is likely to contribute to the high clearance of DUBA from the systemic circulation.

Linker Optimization. *seco*-DUBA contains two hydroxyl groups, which can each be used for coupling to an antibody via a linker. If the linker is coupled to the hydroxyl group in the alkylating moiety, complete elimination of the linker after linker cleavage at the tumor site would be necessary to liberate the hydroxyl group and allow ring closure to the active *spiro* compound. If linker attachment occurs through the DNA-binding moiety, both noncleavable and cleavable linkers might be acceptable, as was shown[30] for some duocarmycin derivatives similar to *seco*-DUBA. When the linker is coupled to the DNA-binding moiety, the hydroxyl group in the alkylating moiety needs to be protected as well to prevent premature ring closure to the *spiro* compound and subsequent degradation of the antibody-bound duocarmycin to **27** and the antibody-bound DNA-binding moiety. The additional requirement for a protective group when the linker is coupled to the DNA-binding moiety thus implies that in this approach, formation of the *spiro* drug requires two activating steps at the tumor site.

Linker-duocarmycins **29** and **30** (Chart 1) were prepared to evaluate the differences between linkage to the DNA-alkylating unit and linkage to the DNA-binding moiety. Both linker-drugs contain a maleimide group for conjugation to a cysteine thiol group on the antibody, the dipeptide valine-citrulline, which is a substrate for cathepsin B,[47] and two self-elimination spacers in between the dipeptide and *seco*-DUBA. The *p*-aminobenzyl alcohol (PABA) self-elimination spacer is a commonly used self-elimination spacer, which is, for example, present in the linker of brentuximab vedotin and in all other ADCs in the clinic bearing the monomethylauristatin E (MMAE) drug. The bisamine cyclization spacer was incorporated to allow for a carbamate linkage between linker and *seco*-DUBA, as such a linkage is generally more stable than a carbonate linkage, which would be present if only a PABA spacer were used. The *N,N′*-dimethyl cyclization spacer was initially selected, as it had been successfully used in prodrugs before.[48−50] Linker-drug **30** furthermore contains a 4-methylpiperazin-1-ylcarbonyl promoiety, in analogy with MDX-1203, designed to stabilize the *seco*-duocarmycin as long as it is still attached to the antibody and to

DOI: 10.1021/mp500781a
Mol. Pharmaceutics 2015, 12, 1813−1835

Scheme 4. Synthesis of Linker-Drug 30[a]

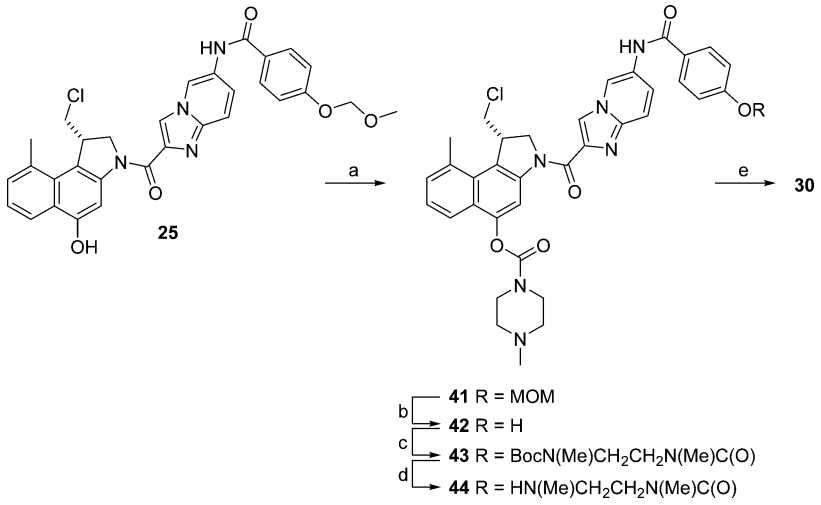

[a]Reagents and conditions: (a) 4-nitrophenyl chloroformate, Et_3N, THF, 0 °C, 1.5 h; then *N*-methylpiperazine, 1 h, 80%; (b) TFA, CH_2Cl_2, 0 °C, 1.5 h; (c) 4-nitrophenyl chloroformate, Et_3N, THF, 0 °C, 3 h; then **38**, 1 h, 38% (2 steps); (d) TFA, CH_2Cl_2, 0 °C, 40 min; (e) **37**, Et_3N, DMF, 0 °C to room temperature, 2 h, 47%.

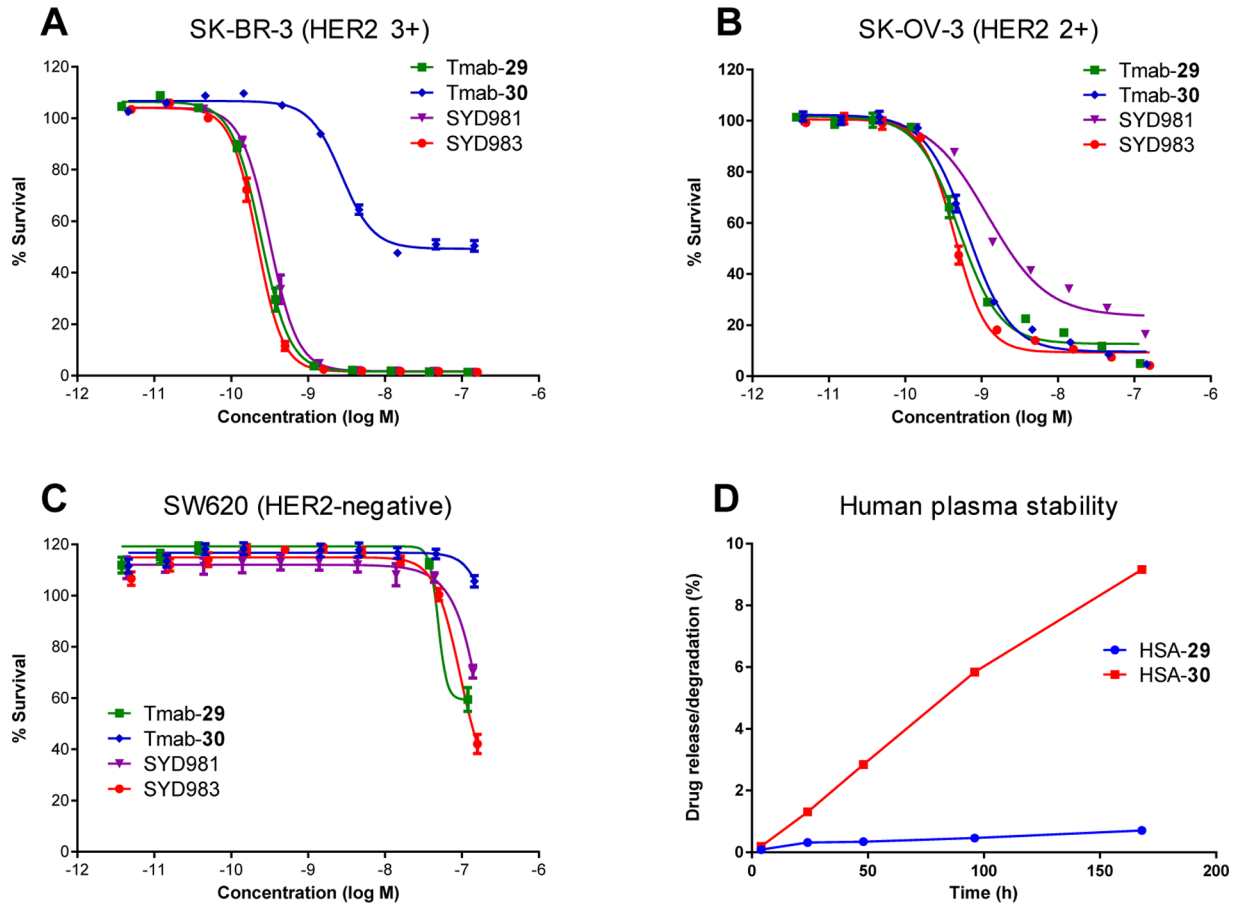

Figure 3. (A–C) Comparison of cytotoxic activities of ADCs Tmab-**29**, Tmab-**30**, SYD981, and SYD983 in SK-BR-3 (A), SK-OV-3 (B), and SW620 (C) cell lines after 144 h of incubation. (D) Human plasma stability of HSA-conjugated **29** and **30**. Release and/or degradation of the conjugated drug moiety were quantified by detection of unconjugated DUBA and DNA-alkylating unit **27**. Percentages are likely underestimated due to the limited stability of DUBA and **27** in plasma.

release the drug through an esterase-mediated cleavage inside the cell.[51,52]

Linker-drug **29** was prepared according to the route depicted in Scheme 3. The linker building block was synthesized by starting with a condensation reaction between commercially available **31** and 2-(2-aminoethoxy)ethanol (**32**) to give alcohol **33**, which was then converted to reactive carbonate **34** through reaction with 4-nitrophenyl chloroformate. Coupling of **34** to

DOI: 10.1021/mp500781a
Mol. Pharmaceutics 2015, 12, 1813–1835

Scheme 5. Protease-Mediated Cleavage of Compounds 46a and 46b, Eventually Leading to Release of DUBA (3b) after Two Consecutive Self-Eliminations

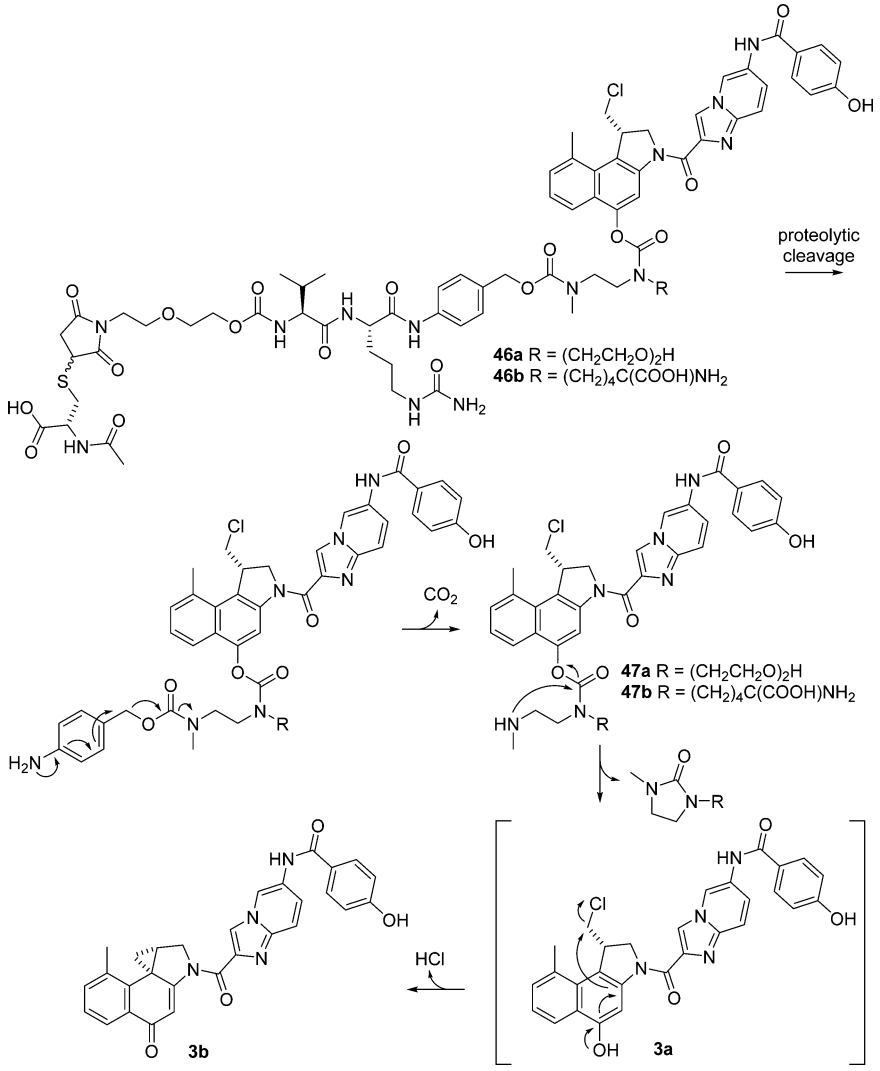

H-Val-Cit-PABA (**35**), prepared according to literature procedures,[53] resulted in formation of linker **36**, which was treated with bis(4-nitrophenyl) carbonate to give activated linker **37**.

The other building block for linker-drug **29**, cyclization spacer-duocarmycin construct **40**, was prepared from MOM-protected duocarmycin **25** in two steps. Consecutive treatment of **25** with 4-nitrophenyl chloroformate and commercially available *tert*-butyl methyl(2-(methylamino)ethyl)carbamate (**38**) gave construct **39**. Removal of the Boc and MOM protective groups in **39** with trifluoroacetic acid (TFA) provided **40** as its TFA salt. Linker-drug **29** was synthesized through reaction of activated linker **37** with cyclization spacer-duocarmycin construct **40** under slightly basic conditions. Under these conditions, self-elimination of the cyclization spacer and resulting formation of **3a** was suppressed.

Linker-drug **30** was synthesized in five steps from linker **37** and alcohol **25** using a reaction sequence largely analogous to that of linker-drug **29** (Scheme 4). Compound **25** was treated consecutively with 4-nitrophenyl chloroformate and 1-methylpiperazine to give carbamate **41**. Ensuing removal of the MOM protective group was followed by reaction of alcohol **42** with 4-nitrophenyl chloroformate and cyclization spacer **38** to give **43**. Removal of the Boc protective group and subsequent coupling of **44** with linker **37** finally afforded linker-duocarmycin **30**.

Linker-duocarmycins **29** and **30** were conjugated to trastuzumab following partial reduction of the interchain disulfide bonds of trastuzumab using tris(2-carboxyethyl)-phosphine (TCEP) as the reducing agent in such an amount that on average one disulfide bond per antibody was reduced. The resulting ADCs, Tmab-**29** and Tmab-**30**, were obtained with average drug-to-antibody ratios (DARs) of approximately 2, as determined by hydrophobic interaction chromatography (HIC).

Tmab-**29** and Tmab-**30** were evaluated for in vitro cytotoxicity in the SK-BR-3, SK-OV-3, and SW620 cell lines. Both ADCs demonstrated cytotoxic activity that was dependent on HER2 expression (Table 1 and Figure 3A–C), as no significant activity was observed for both ADCs against the HER2-negative SW620 cell line. While Tmab-**29** showed subnanomolar activity against the SK-BR-3 and SK-OV-3 cell lines with 90–100% efficacy, Tmab-**30** was only equally potent and efficacious against the SK-OV-3 cell line and considerably less potent against the SK-BR-3 cell line.

Both ADCs were also incubated with SW620 cells in the presence of 1% human or mouse plasma in order to assess

DOI: 10.1021/mp500781a
Mol. Pharmaceutics 2015, 12, 1813–1835

plasma stability. If the linker is unstable in plasma, this could lead to release of the active drug and, consequently, increased cytotoxicity against SW620 cells in the presence of plasma. This assay would not detect degradation pathways that do not lead to release of the active drug.

In the presence of 1% mouse plasma, the linker-drug in Tmab-**29** proved less stable than that in Tmab-**30**. On the basis of the IC_{50} values of 0.46 nM for Tmab-**29** (expressed in drug equivalents) in the presence of mouse plasma, ±100 nM for Tmab-**29** in the absence of mouse plasma, and 0.09 nM for *seco*-DUBA, a significant amount of conjugated drug was released in the six-day assay. In the presence of 1% human plasma, both ADCs did not seem to release any considerable amount of drug within the six-day assay as IC_{50} values were at least 450-fold higher than that of *seco*-DUBA.

In a separate assay, linker-drugs **29** and **30** were incubated in human plasma and release of degradation products was followed over time. When linker-drugs **29** and **30** were added to human plasma, almost instantaneous conjugation to human serum albumin (HSA) took place, complete conversion was observed within 5 min, and therefore stability of HSA-conjugated **29** and **30** was in fact assessed. Quantities of DUBA and DNA-alkylating unit **27** were measured over time as a measure of plasma stability. Results clearly showed that HSA-**29** was highly stable in human plasma, in line with the data from the cellular assay, whereas HSA-**30** was shown to degrade significantly (Figure 3D). Only formation of DNA-alkylating unit **27** was detected. As it was shown separately that the total measurable amount of DUBA and **27** slowly decreased over time after incubation of DUBA in plasma, absolute quantities of DUBA and **27** that were formed after incubation of linker-drugs **29** and **30** could not be determined accurately.

The plasma stability and cytotoxicity assays made clear that linker-drug **30**, being relatively unstable in human plasma and, at least in SK-BR-3 cells, not sufficiently cytotoxic, is outperformed by linker-drug **29** and that linking through the DNA-binding moiety, like in **30**, is thus disfavored over linking to the DNA-alkylating moiety, like in **29**. As no other promoieties showing substantially improved properties could be identified and it was considered an advantage that only one enzymatic cleavage step would be required to release the drug, we decided to move forward with the concept of linking to the DNA-alkylating moiety.

The relatively low stability of Tmab-**29** in mouse plasma was found to be caused by rodent-specific carboxylesterase 1c (CES1c).[43] Although this enzyme is not expressed in man or cynomolgus monkey, optimization of mouse plasma stability was considered useful to enable a better translation of observed efficacy in mouse models. As studies indicated that CES1c cleaves the carbamate linkage between duocarmycin and linker, a large series of linker-duocarmycins with different substituents on the nitrogen atom of the linking carbamate group was synthesized and evaluated. From this series, linker-duocarmycins **2** (Figure 1) and **45** (Chart 1) were selected for more extensive evaluation.

Both linker-drugs were prepared analogously to **29**.[54] The most notable difference was the requirement for 1-hydroxybenzotriazole as a catalyst in the coupling reaction between the Boc-protected cyclization spacer and the 4-nitrophenyl carbonate of **25**, likely due to the lower reactivity of the amine as a consequence of steric congestion. Furthermore, the presence of the amino acid group in the cyclization spacer of linker-drug **45** required a slightly different protective group strategy. The synthesis of **45** was in general somewhat more laborious than that of linker-drug **2**, and the final steps of the synthesis of linker-drug **45** proceeded with somewhat lower yields.

Linker-duocarmycins **2** and **45** were conjugated through their maleimide group to *N*-acetylcysteine, serving as an antibody surrogate, to give compounds **46a** and **46b**, respectively (Scheme 5). Both **46a** and **46b** were efficiently cleaved by cathepsin B at pH 5 at a similar rate, as monitored by formation of cyclization spacer-duocarmycin compounds **47a** and **47b** (data not shown). Self-elimination of the cyclization spacers in **47a** and **47b** at pH 7.4 and 25 °C occurred readily with half-lives of 27 and 37 min, respectively. Half-lives at pH 7.4 and 37 °C were even considerably shorter. As expected, half-lives at pH 5 and 37 °C were longer, being approximately 10 h for both cyclization spacers.

Linker-drugs **2** and **45** were conjugated to trastuzumab following the same procedure as for Tmab-**29**. Tmab-**2** (SYD983) and Tmab-**45** (SYD981) were obtained with average DARs of approximately 2, as confirmed by HIC. Percentages of HMW species, as determined by size exclusion chromatography (SEC), were 1.8 and 3.0% for SYD983 and SYD981, respectively, slightly lower than the percentage of HMW species for Tmab-**29** (4.1%), as was anticipated based on the less lipophilic nature of the substituents in the cyclization spacer.

Both ADCs were evaluated for cytotoxicity in the same three cell lines as Tmab-**29** (Table 1). SYD983 was slightly more potent than SYD981 against the HER2-positive cell lines SK-BR-3 (0.22 nM vs 0.31 nM) and SK-OV-3 (0.44 nM vs 1.20 nM). Both were significantly less active against the HER2-negative SW620 cell line.

In vitro plasma stability of SYD983 and SYD981 was assessed by incubating the ADCs in mouse, rat, monkey, and human plasma. SYD981 demonstrated half-lives ranging from 39 to 291 h, while SYD983 showed half-lives between 6 and 252 h (Table 2). Half-lives of conjugated antibody were determined with a sandwich ELISA assay in which ADCs were captured with an antidrug antibody and detected with an anti-idiotype antibody. All conjugates that contained at least one drug were detected. Conjugated antibody half-lives in plasma were mainly driven by linker-duocarmycin degradation instead of degradation of the antibody component, as a sandwich ELISA assay to detect total antibody, that is, conjugated and unconjugated antibody, using anti-idiotype antibodies for both capture and detection, showed that 75−92% of antibody was remaining after 7 days of incubation in mouse, rat, monkey, or human plasma.

Table 2. Half-Lives of Conjugated Antibody (SYD983 Equivalents) in Mouse, Rat, Monkey, and Human Plasma for ADCs SYD981, SYD982, SYD983, and SYD984

	plasma half-life (h)			
compd	mouse	rat	monkey	human
SYD981 (Tmab-**45**, DAR 2)	39	74	290	291
SYD982 (Tmab-**2**, DAR 1)	4	6	245	278
SYD983 (Tmab-**2**, DAR 2)	6	10	252	241
SYD984 (Tmab-**2**, DAR 3)	10	22	>336	>336

Thus, especially in mouse and rat plasma, SYD981 proved significantly more stable than SYD983. These results were confirmed in a cellular assay, which showed that cytotoxic

DOI: 10.1021/mp500781a
Mol. Pharmaceutics 2015, 12, 1813−1835

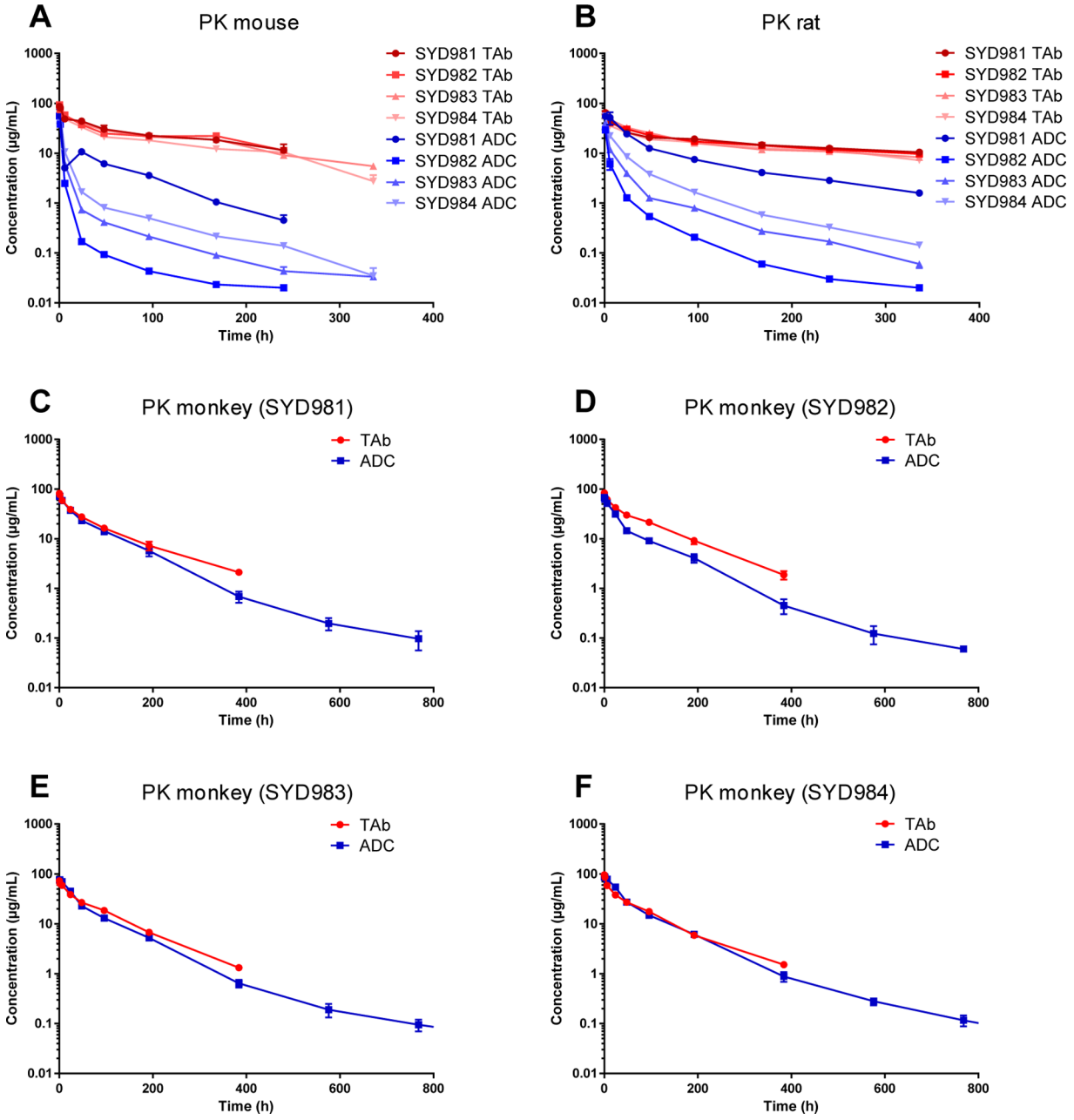

Figure 4. (A,B) Mean total antibody (TAb) and conjugated antibody (ADC, SYD983 equiv) plasma concentrations in female Balb/c mice (A) and Sprague−Dawley rats (B) after a single intravenous bolus injection of SYD981, SYD982, SYD983, or SYD984 at 5 mg/kg (mice) or 3 mg/kg (rats) (n = 3, ±SEM). (C−F) Mean TAb and ADC (SYD983 equiv) plasma concentrations in female cynomolgus monkeys after a single intravenous bolus injection of SYD981 (C), SYD982 (D), SYD983 (E), or SYD984 (F) at 3 mg/kg (n = 3, ±SEM).

activity in the HER2-negative SW620 cell line in the presence of 1% mouse plasma was considerably higher for SYD983 (IC_{50} = 0.93 nM) than for SYD981 (IC_{50} = 3.95 nM), while no significant activity was observed for both ADCs in the presence of 1% human plasma (Table 1).

In vivo PK data for SYD981 and SYD983 were generated in healthy female Balb/c mice (Figure 4A), Sprague−Dawley rats (Figure 4B), and cynomolgus monkeys (Figure 4C,E). The in vivo PK results were well in line with the in vitro plasma stability data. Exposure to conjugated antibody, expressed in SYD983 equivalents, was about three times lower for SYD983 than for SYD981 in female Balb/c mice. For both ADCs, exposure to total antibody was considerably higher, indicating substantial degradation of both ADCs. PK profiles in female Sprague−Dawley rats were similar to those in Balb/c mice, although the ratio between total antibody exposure and conjugated antibody exposure was somewhat smaller for both ADCs. In cynomolgus monkeys, both ADCs demonstrated a very similar PK profile, and conjugated antibody exposure was very close to total antibody exposure, indicating that linker-drug degradation was very limited and that clearance of intact ADC was mainly responsible for the gradual decrease of plasma concentrations of conjugated antibody and total antibody over time.

In line with the slightly higher stability of SYD981 in mouse and rat plasma in vitro and in vivo, the tolerability and toxicity profile of SYD981 was slightly better than that of SYD983 in these species (data not shown). However, the limited plasma

DOI: 10.1021/mp500781a
Mol. Pharmaceutics 2015, 12, 1813−1835

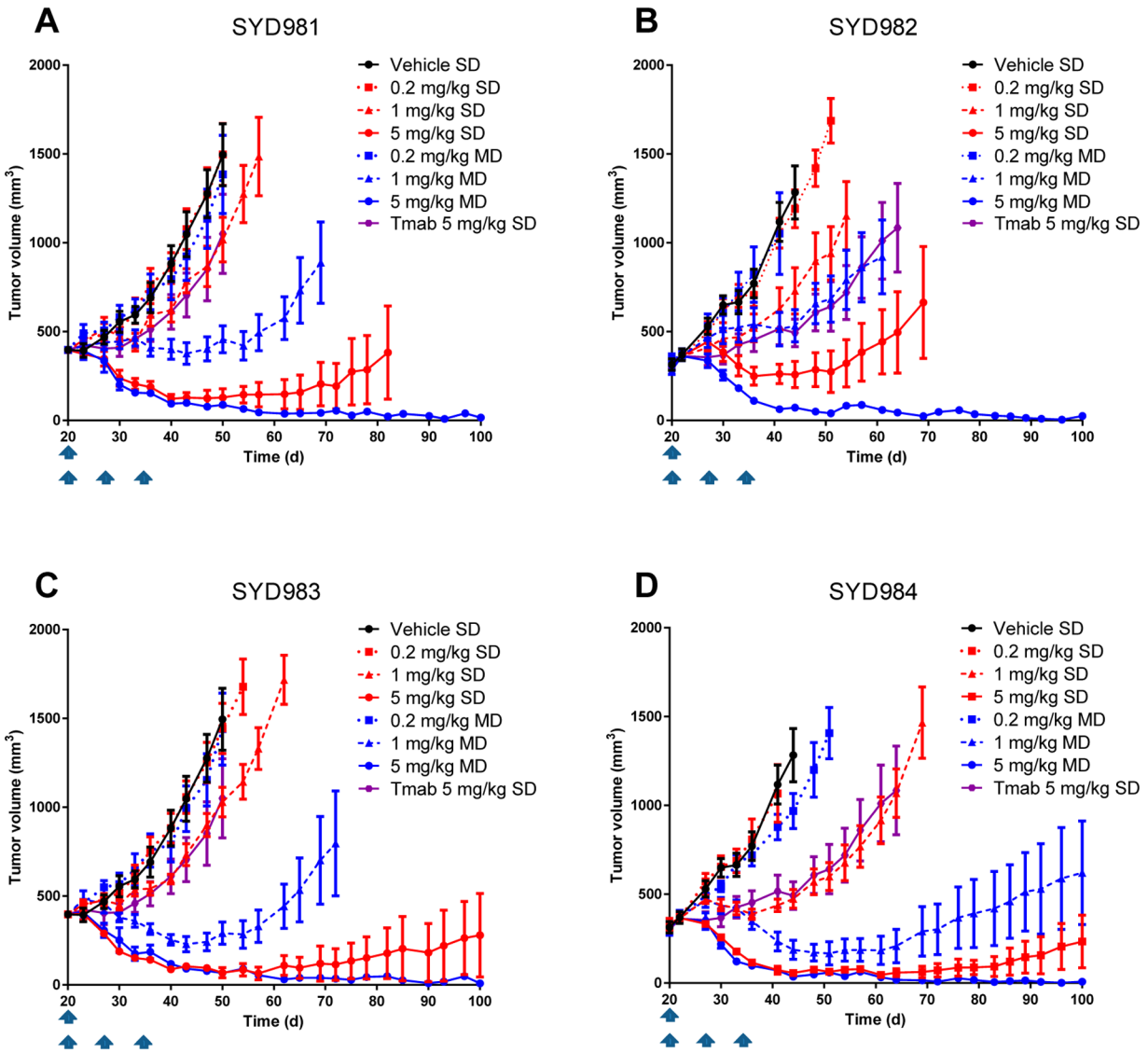

Figure 5. Antitumor activity of ADCs SYD981 (A), SYD982 (B), SYD983 (C), and SYD984 (D) in Balb/c nu/nu mice bearing BT-474 xenografts. Antitumor activity was compared to vehicle and trastuzumab (Tmab). Mice (n = 8 per group) were treated intravenously on the day(s) indicated by the arrow(s) on the x-axis (SD = single dose, MD = multiple doses).

stability of either linker-drug in rodents indicates that these species are of limited value in the quantitative risk assessment for man, where high stability is expected based on human plasma stability data.

In vivo efficacy of the ADCs was assessed in Balb/c nu/nu mice bearing breast carcinoma BT-474 xenografts. In vitro, SYD981 and SYD983 demonstrated IC_{50} values of 0.15 and 0.06 μg/mL, respectively, against the BT-474c cell line, the same subclone as used for the xenograft studies. In the xenograft study, both ADCs were dosed intravenously either once or three times (days 0, 7, and 14) at 0.2, 1, and 5 mg/kg (Figure 5A,C). Both ADCs showed clear dose−response relationships, especially for the multidose regimens. Durable remissions were observed for both SYD981 and SYD983 at 5 mg/kg (qwx3), while tumor growth delay was observed for both 1 mg/kg (qwx3) groups. Mice treated with 0.2 mg/kg (qwx3) did not show a significant effect on tumor growth compared to vehicle. From the groups that received a single dose of ADC, only both 5 mg/kg groups were significantly different from the vehicle group and showed nearly complete tumor regression followed by tumor regrowth. Thus, antitumor activities of SYD983 and SYD981 were, at least in this xenograft model, very comparable, which could be explained by the lower ADC exposure for SYD983, counteracted by the somewhat higher potency of SYD983.

On the basis of the preclinical profiles of SYD981 and SYD983, the more straightforward synthesis of linker-drug **2**, and the lower tendency of SYD983 to form HMW species, linker-drug **2** was selected as the lead linker-drug.

Average DAR. We next set out to determine the optimum DAR. Conjugates of trastuzumab and **2** with average DARs of about 1 (SYD982) and 3 (SYD984) were prepared analogously to SYD983 using different amounts of TCEP. The ADCs were then compared to SYD983 for physicochemical and preclinical properties.

Percentages of HMW species in SYD982, SYD983, and SYD984 were 1.3, 2.4, and 6.0%, respectively. As a consequence of the random conjugation approach, percentages of unconjugated antibody in the ADCs decreased from approximately 60% for SYD982 to 10% for SYD984, while the percentages for

DOI: 10.1021/mp500781a
Mol. Pharmaceutics 2015, 12, 1813−1835

the total of DAR6 and DAR8 species increased from approximately 2% for SYD982 to 10% for SYD984. Despite the presence of different amounts of HMW species and the different percentages for the individual DAR species, a short-term stability study, in which ADCs were stored for 4 weeks at temperatures up to 40 °C, could not differentiate between the ADCs. No significant differences were observed when the ADCs were analyzed for changes in solubilized content, amount of HMW species, average DAR, individual DAR species, onset temperature for aggregation, melting temperature, charged species, and HER2 binding (data not shown).

Plasma stability of SYD982 and SYD984 was comparable to that of SYD983. Conjugated antibody half-lives for SYD982 were between 4 and 278 h, while half-lives for SYD984 ranged from 10 to over 336 h (Table 2). Half-lives for conjugated antibody were, as expected, rather short in rodent plasma, but comparable to total antibody half-lives in monkey and human plasma. Conjugated antibody half-lives increased in the series SYD982 < SYD983 < SYD984, which was anticipated, because more drug has to be removed from a higher-loaded species before it is no longer detected as a conjugated antibody. Half-lives of total antibody were similar for SYD982 and SYD983 in plasma from all species. Half-lives of total antibody for SYD984 in mouse and rat plasma were slightly lower than for SYD983, while they were comparable to those for SYD983 in monkey and human plasma.

In vivo PK data for SYD982 and SYD984 were generated following single intravenous bolus injections of SYD982 and SYD984 in Balb/c mice (Figure 4A), Sprague–Dawley rats (Figure 4B), and cynomolgus monkeys (Figure 4D,F), and results were compared to the data for SYD983. In line with the in vitro plasma stability data, exposure to conjugated antibody in rodents was highest for SYD984 and lowest for SYD982. In cynomolgus monkeys, time–concentration curves for conjugated antibody and total antibody were very similar, indicative of a high in vivo stability of the ADCs. In all species, exposure to total antibody tended to be somewhat lower for SYD984 than for SYD982 and SYD983, which may be indicative of a slightly faster clearance of the intact (higher DAR) ADC species in SYD984 from circulation.

SYD982 and SYD984 were also evaluated for in vivo efficacy in the BT-474 xenograft model (Figure 5B,D). Efficacy clearly depended on drug load. Like SYD983, SYD982 and SYD984 showed a clear dose–response relationship, but at an equivalent antibody dose SYD984 was clearly the most efficacious and SYD982 the least efficacious of the three ADCs. These data were confirmed in vitro when cytotoxicity against the BT-474c cell line was assessed. SYD982 and SYD984 had IC_{50} values of 0.13 and 0.04 μg/mL, respectively, which bracket the value found for SYD983 (0.06 μg/mL).

SYD982, SYD983, and SYD984 were well-tolerated in female cynomolgus monkeys up to two dosages of 30 mg/kg 24 days apart. Clinical, clinical pathology, and histopathological effects observed were all mild and transient, as previously reported for SYD983,[43] and comparable in nature for all three ADCs. However, the intensity of the effects in general increased with dose and increasing average DAR. For example, microscopic examination of skin sections revealed hyperpigmentation of the extremities as one of the most sensitive and quantitative effects, and the degree of hyperpigmentation was highest for SYD984. Notably, peripheral neuropathy, assessed by clinical signs and histopathology, and thrombocytopenia were not observed for any of the ADCs up to 30 mg/kg for two cycles.

On the basis of the estimated efficacy–safety windows of SYD982, SYD983, and SYD984, none of the ADCs could be disqualified. From a physicochemical point of view, however, SYD984 was disfavored because of the higher amount of HMW species. We considered that fractionation of SYD983 to remove the unconjugated antibody and the higher-loaded DAR6 and DAR8 species could result in an ADC outperforming any of the unfractionated ADCs.

Fractionation of SYD983 was carried out with preparative HIC using a resin with a relatively low hydrophobicity. Unconjugated antibody did not bind to the resin under the conditions applied and eluted in the flow-through fraction. The lower DAR species were then eluted with elution buffer that did not contain organic cosolvent. The higher DAR species remained largely bound to the resin until the column was stripped (Figure 6). The fractionated ADC, obtained in approximately 60% yield, was designated SYD985. It is a mixture consisting of about 95% DAR2 and DAR4 species in an approximate 2:1 ratio and has an average DAR of about 2.8. In this respect, SYD985 is much more homogeneous than SYD984, while having a similar average DAR.

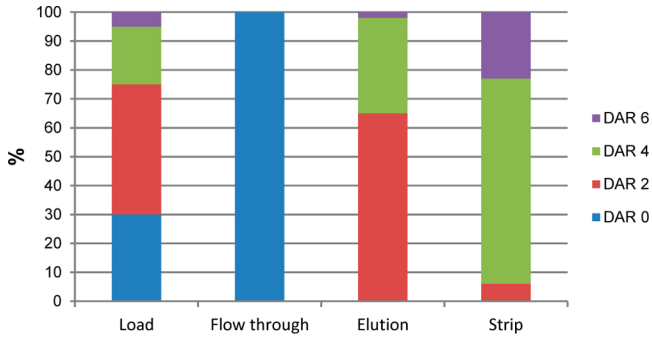

Figure 6. Composition of fractions obtained after preparative HIC of SYD983. The fraction elution represents SYD985.

SYD985 was extensively evaluated preclinically, comparing favorably to its unfractionated predecessor, SYD983.[43] It was also demonstrated to have several favorable pharmacological characteristics with respect to ado-trastuzumab emtansine.[55] Hence, SYD985 was selected for clinical evaluation, and Phase I clinical evaluation recently started.

DISCUSSION

Most of the ADCs that are currently on the market or in clinical development contain drugs that belong either to the class of maytansinoids or to the class of auristatins. Both drug classes inhibit tubulin polymerization, a process that is essential for mitosis, thus inhibiting cell division and eventually inducing apoptosis. The tubulin binder-based ADCs currently in the clinic have several toxicities in common, despite the fact that the ADCs bind to different targets. The nature of the toxicities is in line with the expected adverse effect profile of tubulin inhibitors, that is, neurotoxicity, neutropenia, lymphopenia, and thrombocytopenia, and this may suggest that these toxicities are related to the rather high systemic (peak) exposure levels of unconjugated drug that occur after administration of the ADCs. Alternatively, the similarities in the toxicity profiles of maytansinoid- and auristatin-based ADCs may be due to common deposition characteristics of the ADCs, which are independent of target binding and distribution of the target.

DOI: 10.1021/mp500781a
Mol. Pharmaceutics 2015, 12, 1813–1835

Either way, off-target toxicities are often dose-limiting, thereby limiting the therapeutic index of the ADCs.

We developed a linker-drug technology based on the duocarmycin class of compounds. Duocarmycins, consisting of a DNA-alkylating and a DNA-binding moiety, exert their cell killing capabilities by binding to the minor groove in DNA and selectively alkylating the N3 of adenine residues. We envisioned that this different mechanism of action could enable the development of ADCs with a different clinical profile, both in terms of indications that could be treated and dose-limiting side effects that would be observed. Linker-drugs were evaluated in ADCs based on the HER2-binding antibody trastuzumab. Linker-drug **2**, which contains the inactivated drug *seco*-DUBA (**3a**), was eventually selected as lead linker-drug and used to develop SYD985, an ADC in which the linker-drugs are conjugated to reduced interchain disulfide bridges, consisting mainly of DAR2 and DAR4 species.

seco-DUBA was identified as an interesting candidate drug from an extensive structure−activity relationship study. The imidazo[1,2-*a*]pyridine core structure of the DNA-binding moiety imposes several favorable properties on *seco*-DUBA, one of which being that it has a pK_a close to 6. This can be exploited during ADC manufacturing and formulation of the ADC by using (slightly) acidic process and formulation buffers. Protonation will enhance water solubility of and repulsion between ADC molecules, which in turn may lead to reduced self-association, a common phenomenon of ADCs,[56] especially when they bear relatively hydrophobic drugs.

Hydrolysis of the amide in DUBA (**3b**), resulting from spirocyclization of *seco*-DUBA, occurred more rapidly in plasma compared to the spirocyclized form of its indole analogue **26**. This is likely due to an increased electrophilicity of the carbonyl carbon as a consequence of the additional inductive effects exerted by the second nitrogen atom. Amide hydrolysis is possibly catalyzed or facilitated by plasma components, as DUBA was found to be hydrolyzed more slowly in buffer at physiological pH. On the basis of separate plasma stability studies with ADCs, it seems plausible that it is the *spiro* form that is hydrolyzed, and not the *seco* form, as amide hydrolysis of the antibody-bound drug, trapped in its inactive *seco* form through linker attachment to the hydroxyl group in the alkylating moiety, was not detected. Vinylogous amide conjugation in *spiro* compounds with an alkylating moiety similar to that in DUBA was shown[57] to lengthen the amide C−N bond and allow for amide hydrolysis with lithium hydroxide under unusually mild conditions. Similarly, DUBA may be more sensitive than its (conjugated) *seco* analogue toward hydrolysis in buffer at physiological pH and in plasma because of vinylogous amide conjugation. The in vivo half-life of DUBA in Wistar rats was found to be only 1.1 h. This is considerably shorter than half-lives reported for MMAE (5.6 h in rats[58]) and DM1 (6.3 h at 0.1 mg/kg in Sprague−Dawley rats[59]), representative drugs from the currently most widely explored drug classes for ADCs and the drugs in brentuximab vedotin and ado-trastuzumab emtansine, respectively.

Linkage of *seco*-DUBA to cysteine thiols of partly reduced trastuzumab via a linker connected to its DNA-binding moiety (Tmab-**30**) led to lower in vitro cytotoxicity in SK-BR-3 cells and reduced human plasma stability compared to linkage via the DNA-alkylating unit (Tmab-**29**). Both observations should likely be attributed to the 4-methylpiperazin-1-ylcarbonyl promoiety that was used to block the hydroxyl group in the alkylating moiety of Tmab-**30** to prevent premature spirocyclization and degradation of the antibody-bound drug. This promoiety has also been applied in KW-2189,[51] a duocarmycin prodrug that failed in Phase II clinical trials,[26] and in duocarmycin-based ADC MDX-1203,[31] and was designed to be cleaved by carboxylesterases inside the cell.[52] The lower plasma stability of Tmab-**30** could be explained by a mechanism in which (enzyme-catalyzed) removal of the promoiety is followed by spirocyclization and subsequent hydrolysis of the amide bond in the antibody-bound drug, leading to loss of the DNA-alkylating unit from the ADC. Conversely, inefficient removal of the promoiety in SK-BR-3 cells may be responsible for the reduced cytotoxic activity in SK-BR-3 cells. Therefore, as intracellular levels of carboxylesterase appear to be dependent on the cell line and carboxylesterase seems also present in human plasma, the 4-methylpiperazin-1-ylcarbonyl promoiety seems unsuitable for use in an ADC. As no alternative promoieties could be identified with substantially improved properties, linking via the DNA-binding moiety was abandoned as a strategy.

Linking to the DNA-alkylating moiety in **3a** resulted in excellent stability in monkey plasma for all ADCs that were evaluated. Furthermore, ADCs SYD983, based on linker-drug **2**, and SYD981, based on linker-drug **45**, were shown to have conjugated antibody exposures in cynomolgus monkey that were close to that of total antibody, indicative of high stability of the intact ADC. Thus, in vitro monkey plasma stability translated well to in vivo PK in monkey. It is therefore expected that the excellent stability observed in human plasma will translate into high exposure of intact ADC in patients as well. The slightly faster clearance of conjugated antibody compared to total antibody after dosage of SYD983 or SYD981 to monkeys is a commonly observed phenomenon for ADCs and could, for example, be due to slow linker-drug degradation by plasma enzymes or maleimide exchange.[60,61] The latter comprises transfer of the complete linker-drug moiety through a retro-Michael reaction from the antibody to another molecule with a thiol group, such as albumin or glutathione.

In mouse and rat plasma, SYD983 and SYD981 were less stable. This has been attributed to the presence of rodent-specific CES1c, as in plasma from CES1c knockout mice, SYD983 has a stability comparable to that in cynomolgus monkey and human plasma.[43] Increased stability of SYD983 in the absence of CES1c has been confirmed in vivo in CES1c knockout mice.[55] As cyclization spacer-duocarmycin intermediates were not observed in plasma stability studies, CES1c likely cleaves the carbamate linkage between cyclization spacer and duocarmycin payload.

SYD981 was somewhat more stable than SYD983, but in vitro cytotoxicity was slightly better for SYD983, resulting in in vivo efficacies in a BT-474 xenograft model that were comparable. As both ADCs contain the same drug, different tumor cell pharmacokinetics could account for the difference in in vitro cytotoxicity. Furthermore, differences in pharmacokinetics, for example, differences in linker metabolism in circulation, may exist that cannot be detected with the current ELISA assay to detect conjugated antibody, as this assay specifically detects the duocarmycin component.

The in vitro cytotoxicity data of linker-drug **2**-based ADCs SYD982, SYD983, and SYD984, having average DARs of approximately 1, 2, and 3, respectively, show that potency in BT474c cells increases with increasing DAR when IC_{50} values are expressed in antibody equivalents. When expressed in drug equivalents, however, IC_{50} values are comparable, suggesting

DOI: 10.1021/mp500781a
Mol. Pharmaceutics 2015, 12, 1813−1835

that the total amount of drug that is released inside the BT474c cells correlates with the extracellular concentration of antibody-bound payload. Similarly, SYD984 was shown to be the most efficacious ADC in the BT-474 xenograft model on a mg/kg basis, but the three ADCs are more comparable in terms of efficacy when dosages are expressed in drug equivalents. From an efficacy point of view, SYD984 may be favored over SYD983 and SYD982 because (i) a lower dose of SYD984 is needed to reach a certain level of efficacy; (ii) SYD984 is potentially more effective in the treatment of tumors that express low copy numbers of HER2 and are only able to shuttle a limited number of ADC molecules into the cell; and (iii) SYD984 contains a lower amount of unconjugated trastuzumab, which can compete with conjugated trastuzumab for HER2 binding, thereby potentially lowering antitumor activity.

Results from a dose-range finding toxicity and pharmacokinetic study in cynomolgus monkeys showed minimal differences between SYD982, SYD983, and SYD984 up to the highest dose tested (30 mg/kg, q24dx2). Although toxicities were generally somewhat more intense at higher average DAR, effects were generally mild and reversible. Dependent on the type of tissue affected and whether or not there is (low) expression of HER2, increased toxicity in the series SYD982 < SYD983 < SYD984 may, for instance, be caused by augmented drug exposure, enhanced exposure to higher-loaded conjugates, or reduced exposure to unconjugated antibody. PK profiles in cynomolgus monkeys showed that exposure to total antibody was slightly lower for SYD984 than for SYD982 and SYD983, which could be explained by a faster clearance of intact higher DAR species from circulation.[62] In contrast, exposure to conjugated antibody was highest for SYD984. This is in line with expectations because more time is needed to fully deconjugate the higher-loaded antibody.

SYD985, obtained through HIC fractionation of SYD983, consists of about 95% DAR2 and DAR4 species in an approximate 2:1 ratio and has an average DAR of about 2.8. It is comparable to SYD984 in terms of average DAR, but it is considerably more homogeneous and contains significantly lower amounts of unconjugated antibody and DAR6 and DAR8 species. Absence of the higher DAR species is considered advantageous as these species are likely to be more rapidly cleared, more toxic, and more prone to aggregation,[62] while absence of unconjugated trastuzumab prevents competition at the level of receptor binding and internalization.

In conclusion, anti-HER2 ADC SYD985 was selected as lead clinical candidate following extensive linker-duocarmycin structure−activity studies, in which both drug and linker components were optimized and the composition of the ADC in terms of average DAR and DAR species was improved. SYD985 recently entered clinical Phase I evaluation.

EXPERIMENTAL SECTION

General. The protocols for the synthesis of H-Val-Cit-PABA[53] and linker-drugs **2** and **45**,[54] the conjugation of linker-drugs to trastuzumab,[43] and the HIC purification of SYD983[43] have been described elsewhere. The SEC and HIC methods used for characterization of ADCs, the ELISA methods to quantify total antibody and conjugated antibody, the methods used for data analysis of in vitro data, and the protocols for measuring in vitro plasma stability and carrying out the in vivo efficacy and safety studies have been described before.[43] Linker-drugs were purified by preparative HPLC on a Waters SunFire Prep C18 OBD column (5 μm, 19 × 150 mm) using acetonitrile and 0.1% TFA in water as the eluents. Purity of compounds was assessed by HPLC and was ≥95% in all cases. Optical rotation was recorded on a PerkinElmer 241 polarimeter. Enantiomeric excess was determined by HPLC on a Daicel Chiralcel OD-H column (5 μm, 4.6 × 250 mm; *n*-heptane/isopropyl alcohol, 99:1, v/v; flow rate, 0.8 mL/min). NMR spectra were recorded on a Bruker AVANCE400 (400 MHz for ^{1}H; 100 MHz for ^{13}C) or Bruker AVANCE300 (300 MHz for ^{1}H; 75 MHz for ^{13}C) spectrometer. Chemical shifts are reported in ppm relative to tetramethylsilane as an internal standard. Silica gel for column chromatography (40−63 μm, 60 Å) was obtained from Screening Devices. All solvents used were reagent-grade or HPLC-grade.

Compound Characterization. *Methyl 4-Hydroxy-8-methyl-2-naphthoate (**7**).* 2-Methylbenzaldehyde (**4**) (144 mL, 1.25 mol) and dimethyl succinate (**5**, 319 g, 2.18 mol) in methanol (400 mL) were treated with NaOMe (87.8 g, 1.63 mol) at 65−80 °C for 1 h. The mixture was cooled to 20 °C, neutralized with 3 M hydrochloric acid, and diluted with water. Unreacted **5** was removed by extraction with CH_2Cl_2. The mixture was acidified with 3 M hydrochloric acid, and the product was extracted into CH_2Cl_2. The extract was dried with $MgSO_4$, filtered, and concentrated, providing a 9:1 mixture of (*E*) isomer **6a** and (*Z*) isomer **6b**. The crude product was dissolved in THF (1 L), and the solution was treated with TFAA (165 mL, 1.19 mol) at reflux temperature until complete conversion to **7**. The reaction mixture was neutralized with an aqueous K_2CO_3 solution. The product was extracted with EtOAc. The organic layer was dried with $MgSO_4$, filtered, and concentrated, and the residue was crystallized by cooling to −5 °C. The white-yellow crystals were filtered, washed with acetonitrile, and dried, providing alcohol **7** (112 g, 42%).

^{1}H NMR ($CDCl_3$, 300 MHz): δ = 2.74 (3H, s, 8-CH_3), 3.99 (3H, s, CH_3O), 6.07 (1H, s, OH), 7.38 (1H, d, H7), 7.48 (1H, dd, H6), 7.53 (1H, s, H3), 8.12 (1H, d, H5), 8.37 (1H, s, H1). ^{13}C NMR (DMSO-d_6, 100 MHz): δ = 19.7 (8-CH_3), 52.7 (CH_3O), 107.0 (C3), 117.7 (C1), 120.81 (C5), 127.3 (C6), 127.5 (C4a, C2), 128.3 (C7), 133.1 (C8a), 135.7 (C8), 154.5 (C4), 167.1 (C═O).

*4-(Benzyloxy)-8-methyl-2-naphthoic Acid (**9**).* Alcohol **7** (83 g, 0.38 mol) was treated with benzyl chloride (46.4 mL, 403 mmol) in DMF (330 mL) at 80 °C in the presence of K_2CO_3 (74.3 g, 537 mmol). When the reaction was complete, the mixture was cooled and diluted with CH_2Cl_2 and water. The layers were separated, and the organic layer was concentrated. The residue, comprising methyl 4-(benzyloxy)-8-methyl-2-naphthoate (**8**), was dissolved in toluene (500 mL) and methanol (650 mL), and the resultant solution was treated with a 4 M aqueous NaOH solution (750 mL) under reflux for 2 h. Water (2.9 L) was added in several portions, and methanol and toluene were removed by distillation. Crude **9** was precipitated by addition of 4 M hydrochloric acid (330 mL), the suspension was cooled to 10 °C, and the precipitate was filtered off, washed with cold water, collected, and dried. Crude **9** was crystallized from toluene to give off-white crystals. Crystals were filtered, washed with toluene, and dried to give **9** (95.6 g, 82%).

^{1}H NMR (DMSO-d_6, 300 MHz): δ = 2.69 (3H, s, 8-CH_3), 5.37 (2H, s, CH_2Ph), 7.40−7.60 (8H, m, H_{Ar}), 8.11 (1H, d, H5), 8.29 (1H, s, H1), 13.20 (1H, br s, CO_2H). ^{13}C NMR (DMSO-d_6, 100 MHz): δ = 19.7 (8-CH_3), 70.1 (CH_2Ph), 104.8 (C3), 119.7 (C1), 120.4 (C5), 127.8 (C4a), 127.9 (C2,

DOI: 10.1021/mp500781a
Mol. Pharmaceutics 2015, 12, 1813−1835

C2′), 128.4 (C6), 128.5 (C7), 128.6 (C4′), 129.0 (C3′), 132.7 (C8a), 135.9 (C8), 137.4 (C1′), 154.8 (C4), 168.1 (C═O).

*tert-Butyl (4-(Benzyloxy)-8-methylnaphthalen-2-yl)-carbamate (**10**).* Acid **9** (100 g, 342 mmol) was reacted with diphenylphosphoryl azide (109 g, 397 mmol), *tert*-butyl alcohol (65.9 g, 889 mmol), and Et_3N (52.3 mL, 376 mmol) in toluene (500 mL) at 85 °C for 3 h. After the mixture had been cooled to 30 °C, EtOAc and water were added, and the layers were separated. The organic layer was washed with an aqueous Na_2CO_3 solution and saturated aqueous NaCl, dried with $MgSO_4$, filtered, and concentrated. The residue was triturated with isopropyl alcohol. The solid was filtered off, washed with isopropyl alcohol, and dried to provide **10** (110 g, 88%).

^{1}H NMR (DMSO-d_6, 400 MHz): δ = 1.53 (9H, s, Boc), 2.56 (3H, s, 8-CH_3), 5.34 (2H, s, CH_2Ph), 7.23 (1H, m, H6), 7.30−7.39 (3H, m, H1, H7, H4′), 7.42−7.46 (2H, m, H3′), 7.56−7.59 (2H, m, H2′), 7.82 (1H, s, H3), 7.99 (1H, d, H5), 9.53 (1H, s, NH). ^{13}C NMR (DMSO-d_6, 100 MHz): δ = 20.0 (8-CH_3), 28.6 ($CH_{3,Boc}$), 69.9 (CH_2Ph), 79.6 (C_{Boc}), 100.0 (C3), 103.3 (C1), 120.1 (C5), 121.9 (C4a), 123.4 (C6), 128.0 (C7), 128.1 (C2′), 128.4 (C4′), 129.0 (C3′), 133.1 (C8a), 134.0 (C8), 137.4 (C1′), 138.0 (C2), 153.3 (C═O), 154.9 (C4).

*tert-Butyl (R)-(4-(Benzyloxy)-1-bromo-8-methylnaphthalen-2-yl)(oxiran-2-ylmethyl)carbamate (**12**).* Carbamate **10** (105 g, 289 mmol) was treated with NBS (54.0 g, 303 mmol) in THF (1.7 L) at −10 °C. After completion of the reaction, the reaction was quenched by addition of an aqueous Na_2SO_3 solution followed by a 1 M NaOH solution. EtOAc was added, and the layers were separated. The organic layer was washed with saturated aqueous NaCl, dried with $MgSO_4$, and concentrated to give crude **11** in quantitative yield. Crude **11** was dissolved in THF (330 mL), deprotonated with KO*t*-Bu (42.1 g, 376 mmol) at 10 °C, and alkylated with (*S*)-glycidyl nosylate (89.9 g, 347 mmol) at 25 °C for 3 h. The reaction was quenched by addition of an aqueous NH_4Cl solution, and the mixture was extracted with EtOAc. The organic layer was washed with water and saturated aqueous NaCl. Crude **12** was obtained after evaporation of the solvents. Crystallization from heptane gave **12** (119 g, 82%) as beige crystals.

^{1}H NMR ($CDCl_3$, 400 MHz): δ = 1.32 + 1.34 + 1.57 + 1.59 (9H, multiple s, Boc), 2.47 (1H, m, $CH_{2,epoxide}$), 2.69 (1H, m, $CH_{2,epoxide}$), 3.05−3.46 (5H, m, CH_2N, $CH_{epoxide}$, 8-CH_3), 4.15 (1H, m, CH_2N), 5.22−5.27 (2H, m, CH_2Ph), 6.90 (1H, m, H3), 7.31−7.52 (7H, m, H6, H7, $5H_{Ph}$), 8.34 (1H, m, H5). ^{13}C NMR ($CDCl_3$, 100 MHz): δ = 27.0, 27.1, 28.2, 28.2, 28.5, 28.5, 45.9, 46.1, 46.3, 49.6, 49.7, 50.3, 50.5, 50.7, 60.0, 52.7, 53.6, 70.4, 70.4, 70.5, 80.5, 80.5, 81.1, 107.4, 107.6, 107.7, 107.8, 112.4, 112.7, 113.2, 121.3, 121.3, 125.7, 125.8, 125.8, 127.6, 127.7, 127.8, 128.1, 128.6, 128.7, 132.2, 132.3, 132.3, 132.4, 135.9, 136.0, 136.5, 136.5, 140.0, 140.1, 140.7, 154.2, 154.2, 154.3.

*tert-Butyl (S)-5-(Benzyloxy)-1-(hydroxymethyl)-9-methyl-1,2-dihydro-3H-benzo[e]indole-3-carboxylate (**13**).* Epoxide **12** (103.4 g, 207 mmol) was dissolved in THF (1 L). The solution was cooled to −25 °C under an atmosphere of nitrogen. Then *n*-BuLi (100 mL, 2.5 M in hexanes) was added gradually, while the temperature was kept at −25 to −20 °C. The mixture was stirred for an additional 10 min and then quenched with a saturated aqueous NH_4Cl solution. The mixture was extracted twice with EtOAc (2 × 500 mL). An aqueous solution of *p*-toluenesulfonic acid (12 g of monohydrate in 50 mL of water) was added to the combined organic layers, and the reaction mixture was stirred for 1 h. The reaction was quenched by addition of a 1 M aqueous Na_2CO_3 solution. Layers were separated and the organic layer was washed with saturated aqueous NaCl, dried with $MgSO_4$, and concentrated. Crude **13** was dissolved in CH_2Cl_2 and filtered over silica gel (0.063−0.1 mm, 60 Å). Elution was carried out with CH_2Cl_2 (2.2 L) followed by CH_2Cl_2/EtOAc (2.7 L, 9:1, v/v) and CH_2Cl_2/EtOAc (2.4 L, 4:1, v/v). The fractions containing **13** were combined, the resultant solution was concentrated and dried, and the residue was crystallized from CH_2Cl_2/pentane. Crystals were collected and dried to give alcohol **13** (34.7 g, 40%) as a beige to white solid.

^{1}H NMR (DMSO-d_6, 400 MHz): δ = 1.57 (9H, s, Boc), 2.79 (3H, s, 9-CH_3), 3.07 (1H, m, CH_2OH), 3.52 (1H, m, CH_2OH), 3.87−3.96 (2H, m, H1, H2), 4.23 (1H, m, H2), 5.09 (1H, m, OH), 5.20−5.32 (2H, m, CH_2Ph), 7.23 (1H, m, H7), 7.33 (1H, m, H8), 7.39 (1H, m, H4′), 7.44−7.48 (2H, m, H3′), 7.57−7.59 (2H, m, H2′), 7.84 (1H, br s, H4), 8.07 (1H, d, H6). ^{13}C NMR (DMSO-d_6, 100 MHz): δ = 23.09 (9-CH_3), 28.5 ($CH_{3,Boc}$), 43.9 (C1), 51.8 (C2), 64.0 (CH_2OH), 70.1 (CH_2Ph), 80.9 (C_{Boc}), 97.0 (C4), 116.5 (C9a), 121.3 (C6), 123.1 (C5a), 123.3 (C7), 128.0 (C2′), 128.4 (C4′), 129.0 (C3′), 130.7 (C9a), 131.0 (C8), 132.9 (C9), 137.4 (C1′), 141.7 (C3a), 152.7 (C═O), 155.2 (C5).

*tert-Butyl (S)-5-(Benzyloxy)-1-(chloromethyl)-9-methyl-1,2-dihydro-3H-benzo[e]indole-3-carboxylate (**15**).* Alcohol **13** (17.0 g, 40.5 mmol) was treated with methanesulfonyl chloride (4.08 mL, 52.7 mmol) and Et_3N (14.6 mL, 105 mmol) in CH_2Cl_2 (140 mL) for 90 min at 0−5 °C. The reaction mixture was washed with hydrochloric acid, water, and saturated aqueous NaCl, dried with $MgSO_4$, and concentrated. The residue, comprising the intermediate mesylate, was dissolved in DMF (120 mL), and the solution was treated with LiCl (8.59 g, 203 mmol) at 80 °C for 90 min. After evaporation of DMF, the residue was partitioned between CH_2Cl_2 and water. The layers were separated, and the organic layer was washed with saturated aqueous NaCl, dried with $MgSO_4$, and concentrated. The residue was dissolved in hot heptane (350 mL), and the mixture was treated with activated carbon and filtered. The activated carbon was washed with another portion of heptane. The combined filtrate was cooled to approximately 50 °C, seeded, and kept at this temperature for 1 h. The suspension was cooled to 7 °C over 2 h and stirred for another hour at this temperature. Crystals were filtered, washed with heptane, collected, and dried. Dried crystals were recrystallized from heptane using the procedure described above, giving chloride **15** (11.1 g, 63%; enantiomeric excess, 99.99%).

$[\alpha]^{20}_D$ = −20 (*c* 1.0, $CHCl_3$). ^{1}H NMR (DMSO-d_6, 400 MHz): δ = 1.57 (9H, s, Boc), 2.75 (3H, 9-CH_3), 3.41 (1H, t, H2), 3.73 (1H, m, H2), 4.02 (1H, m, CH_2Cl), 4.14 (1H, m, CH_2Cl), 4.23 (1H, m, H1), 5.24−5.34 (2H, m, CH_2Ph), 7.25 (1H, m, H7), 7.35−7.40 (2H, m, H8, H4′), 7.44−7.47 (2H, m, H3′), 7.55−7.59 (2H, m, H2′), 7.84 (1H, br s, H4), 8.09 (1H, d, H6). ^{13}C NMR (DMSO-d_6, 100 MHz): δ = 22.8 (9-CH_3), 28.5 ($CH_{3,Boc}$), 43.4 (C1), 48.2 (C2), 52.3 (CH_2Cl), 70.1 (CH_2Ph), 81.3 (C_{Boc}), 96.8 (C4), 115.3 (C9b), 121.5 (C6), 123.3 (C5a), 123.6 (C7), 128.0 (C2′), 128.4 (C4′), 129.0 (C3′), 130.7 (C9a), 131.2 (C8), 132.4 (C9), 137.2 (C1′), 142.0 (C3a), 152.4 (C═O), 155.9 (C5).

*Ethyl 6-Nitroimidazo[1,2-a]pyridine-2-carboxylate (**18**).* 5-Nitropyridin-2-amine (**17**, 50 g, 359 mmol) was suspended in ethanol (700 mL), and argon was led through the suspension. Next, ethyl bromopyruvate (**16**, 63 mL, 503 mmol) was added,

DOI: 10.1021/mp500781a
Mol. Pharmaceutics 2015, 12, 1813−1835

and the mixture was stirred for 45 min. The reaction mixture was heated to 85 °C and kept at this temperature for 6 h. Additional ethyl bromopyruvate (13.5 mL, 108 mmol) was added, and the mixture was kept at 85 °C for 16 h. Subsequently, the reaction mixture was cooled and concentrated. Water (300 mL) was added, and the resulting suspension was filtered. The residue was rinsed with diethyl ether and dried to yield **18** (75.0 g, 89%) as a sand-colored solid.

^{1}H NMR (DMSO-d_6, 400 MHz): δ = 1.36 (3H, t, CH_3), 4.36 (2H, q, CH_2), 7.80 (1H, m, H8), 8.05 (1H, m, H7), 8.76 (1H, s, H3), 9.90 (1H, dd, H5). ^{13}C NMR (DMSO-d_6, 100 MHz): δ = 14.7 (CH_3), 61.3 (CH_2), 118.0 (C8), 121.1 (C3, C7), 129.6 (C5), 138.0 (C8a), 138.4 (C2), 144.9 (C6), 162.3 (C═O).

*Ethyl 6-Aminoimidazo[1,2-a]pyridine-2-carboxylate (**19**).* A suspension of ester **20** (20 g, 85 mmol) in methanol (200 mL) was cooled to 0 °C, and 12 M hydrochloric acid (70 mL) was added drop by drop, followed by addition of zinc (22.3 g, 340 mmol) in small portions. The reaction mixture was stirred for 30 min. Next, methanol (140 mL) was added, and the reaction was quenched with concentrated ammonia. The suspension was filtered and the residue washed with methanol (2 × 25 mL). The combined filtrate was concentrated and the residue suspended in a mixture of chloroform (700 mL), water (300 mL), and concentrated ammonia (300 mL, 35% solution). The mixture was stirred until it became clear. Layers were separated, and the water layer was extracted once with chloroform. The combined organic layers were washed with saturated aqueous NaCl, dried with $MgSO_4$, filtered, and concentrated to yield amine **19** (11.8 g, 68%) as a gray-green solid.

^{1}H NMR (DMSO-d_6, 400 MHz): δ = 1.27 (3H, t, CH_3), 4.24 (2H, q, CH_2), 5.12 (2H, br s, NH_2), 6.96 (1H, dd, H7), 7.37 (1H, d, H8), 7.68 (1H, s, H5), 8.32 (1H, s, H3). ^{13}C NMR (DMSO-d_6, 100 MHz): δ = 14.7 (CH_3), 61.3 (CH_2), 106.8 (C5), 117.6 (C3), 118.0 (C8), 123.2 (C7), 134.8 (C2), 137.4 (C8a), 141.7 (C6), 163.4 (C═O).

*6-(4-(Methoxymethoxy)benzamido)imidazo[1,2-a]-pyridine-2-carboxylic Acid (**22**).* To a solution of amine **19** (13.3 g, 64.8 mmol) in DMA (200 mL) were added 4-(methoxymethoxy)benzoic acid (**20**, 11.8 g, 64.8 mmol) and EDC·HCl (14.9 g, 77.7 mmol). The resulting mixture was stirred for 18 h at room temperature. Subsequently, the reaction mixture was concentrated. The residue was dissolved in water (250 mL) and CH_2Cl_2 (250 mL), and the layers were separated. The organic layer was washed with water, dried with $MgSO_4$, and concentrated. The residue was transferred to a filter and rinsed with EtOAc. The intermediate, ethyl 6-(4-(methoxymethoxy)benzamido)imidazo[1,2-*a*]pyridine-2-carboxylate (**21**), was dried under vacuum. After drying was complete, **21** was dissolved in 1,4-dioxane (50 mL) and water (50 mL), and an aqueous 2 M NaOH solution (100 mL) was added. The mixture was stirred at 70 °C for 30 min. Next, the mixture was cooled to room temperature, water was added, and the mixture was acidified with a 4 M hydrochloric acid solution. The resulting suspension was filtered, and the residue was dried to give acid **22** (12.1 g, 55%) as a yellow-brown solid.

^{1}H NMR (DMSO-d_6, 400 MHz): δ = 3.43 (3H, s, CH_3), 5.32 (2H, s, CH_2), 7.18 (2H, d, H3′), 7.67 (1H, m, H7), 7.76 (1H, m, H8), 8.08 (2H, d, H2′), 8.65 (1H, s, H3), 9.47 (1H, s, H5), 10.54 (1H, s, NH). ^{13}C NMR (DMSO-d_6, 100 MHz): δ = 56.3 (CH_3), 94.2 (CH_2), 116.1 (C3′), 117.5 (C7), 118.0 (C5), 119.3 (C3), 124.4 (C8), 127.6 (C1′), 128.2 (C6), 130.2 (C2′), 136.3 (C2), 142.4 (C8a), 160.1 (C4′), 164.3 (C═O), 165.7 (C═O).

*Compound **24**.* Compound **15** (4.50 g, 10.3 mmol) was dissolved in 4 M HCl in dioxane (30 mL), and the solution was stirred for 4 h. A suspension was formed, which was concentrated and dried to yield amine **23** as its HCl salt. This was then dissolved in DMA (80 mL), the solution was cooled to 0 °C, and **22** (3.86 g, 11.30 mmol) and EDC·HCl (5.91 g, 30.8 mmol) were added. The mixture was stirred for 18 h, the temperature slowly being increased to 20 °C. Subsequently, the reaction mixture was concentrated, the crude product was dissolved in CH_2Cl_2/water (1.2 L, 1:1, v/v), and the layers were separated. The organic layer was dried with $MgSO_4$, filtered, and concentrated. The crude product was purified by column chromatography (CH_2Cl_2/methanol, 1:0 to 39:1, v/v). Compound **24** was obtained as a white to gray solid (6.3 g, 93%).

^{1}H NMR (DMSO-d_6, 400 MHz): δ = 2.80 (3H, s, 9-CH_3), 3.41 (3H, s, CH_3O), 3.47 (1H, m, CH_2Cl), 3.78 (1H, m, CH_2Cl), 4.37 (1H, m, H1), 4.62 (1H, m, H2), 5.16 (1H, m, H2), 5.30 (4H, s, CH_2Ph, OCH_2O), 7.18 (2H, m, H3″), 7.31 (1H, m, H7), 7.34−7.40 (2H, m, H8, H4‴), 7.44 (2H, m, H3‴), 7.55−7.59 (3H, m, H2‴, H8′), 7.73 (1H, m, H7′), 7.99 (2H, m, H2″), 8.14 (1H, m, H6), 8.31 (1H, br s, H4), 8.69 (1H, s, H3′), 9.48 (1H, s, H5′), 10.31 (1H, s, NH). ^{13}C NMR (DMSO-d_6, 100 MHz): δ = 22.8 (9-CH_3), 44.7 (C1), 47.9 (CH_2Cl), 55.1 (C2), 56.3 (CH_3O), 70.2 (CH_2Ph), 94.2 (OCH_2O), 98.9 (C4), 116.1 (C3″), 117.3 (C9b), 117.7 (C5′), 118.0 (C7′), 119.6 (C3′), 121.5 (C6), 123.5 (C8′), 124.2 (C7), 124.3 (C5a), 127.7 (C1″), 127.9 (C2′), 128.0 (C2‴), 128.4 (C4‴), 129.0 (C3‴), 130.1 (C2″), 130.3 (C9a), 131.1 (C8), 132.9 (C9), 137.3 (C1‴), 141.3 (C6′), 141.9 (C8a′), 143.3 (C3a), 155.3 (C5), 160.0 (C4″), 162.4 (C═O), 165.6 (C═O).

*Compound **25**.* A suspension of Pd/C (10 wt %, 0.507 g, 0.476 mmol) and ammonium formate (6.01 g, 95.3 mmol) in methanol (20 mL) was heated at 95 °C for 5 min. The mixture was then allowed to cool to room temperature. Subsequently, additional ammonium formate (6.01 g, 95.3 mmol) was added followed by a suspension of compound **24** (6.3 g, 9.53 mmol) in THF (100 mL). The resulting mixture was stirred for 3 h at room temperature. When the reaction was complete, the mixture was filtered over Hyflo. Hyflo was rinsed with THF, and the combined filtrate was concentrated. The crude product was purified by column chromatography (CH_2Cl_2/methanol, 39:1 to 9:1, v/v) to yield compound **25** (4.9 g, 90%) as a dark yellow solid.

^{1}H NMR (DMSO-d_6, 400 MHz): δ = 2.80 (3H, s, 9-CH_3), 3.40−3.47 (4H, m, CH_2Cl, OCH_3), 3.78 (1H, m, CH_2Cl), 4.33 (1H, m, H1), 4.61 (1H, m, H2), 5.09 (1H, m, H2), 5.32 (2H, s, OCH_2), 7.18−7.27 (3H, m, H7, H3″), 7.34 (1H, m, H8), 7.61 (1H, m, H8′), 7.75 (1H, m, H7′), 8.02 (2H, m, H2″), 8.07 (1H, m, H6), 8.14 (1H, br s, H4), 8.70 (1H, s, H3′), 9.48 (1H, s, H5′), 10.35 (1H, s, NH), 10.46 (1H, s, OH). ^{13}C NMR (DMSO-d_6, 100 MHz): δ = 22.9 (9-CH_3), 47.7 (C1), 48.0 (CH_2Cl), 55.1 (C2), 56.3 (OCH_3), 94.2 (OCH_2), 100.8 (C4), 115.7 (C9b), 116.1 (C3″), 117.8 (C5′), 118.0 (C7′), 119.3 (C3′), 122.0 (C6), 123.3 (C7), 123.5 (C8′), 123.8 (C5a), 127.8 (C1″), 127.9 (C2′), 130.1 (C2″), 130.6 (C9a), 130.8 (C8), 132.6 (C9), 141.4 (C6′), 141.9 (C8a′), 143.2 (C3a), 155.1 (C5), 160.1 (C4″), 162.4 (C═O), 165.6 (C═O).

*seco-DUBA (**3a**).* To compound **25** (18 g, 31.5 mmol) were added 4 M HCl in dioxane (480 mL) and 4 M hydrochloric

DOI: 10.1021/mp500781a
Mol. Pharmaceutics 2015, 12, 1813−1835

acid (235 mL). A yellow suspension was formed, which was stirred for 1 h at room temperature. Subsequently, the reaction mixture was concentrated. The residue was suspended in diethyl ether, and the suspension was stirred for 90 min. The mixture was filtered, and the residue was washed with diethyl ether. The solid was dried to give *seco*-DUBA (16.9 g, 95%) as its HCl salt.

^{1}H NMR (DMSO-d_6, 400 MHz): δ = 2.78 (3H, s, 9-CH_3), 3.56 (1H, m, CH_2Cl), 3.78 (1H, m, CH_2Cl), 4.39 (1H, m, H1), 4.57−4.62 (2H, m, H2), 6.93 (2H, m, H3″), 7.24 (1H, m, H7), 7.32 (1H, m, H8), 7.92 (1H, m, H8′), 7.98−8.05 (4H, m, H4, H6, H2″), 8.29 (1H, m, H7′), 9.16 (1H, s, H3′), 9.79 (1H, s, H5′), 10.50 (1H, br s, OH), 10.62 (1H, br s, OH), 10.76 (1H, s, NH). ^{13}C NMR (DMSO-d_6, 100 MHz): δ = 22.4 (9-CH_3), 44.4 (C1), 47.7 (CH_2Cl), 54.0 (C2), 99.8 (C4), 112.9 (C8′), 115.1 (C3″), 115.7 (C9b), 117.6 (C3′), 118.0 (C5′), 121.6 (C6), 123.4 (C7), 123.8 (C5a), 123.9 (C2′, C1″), 129.4 (C7′), 129.9 (C6′), 130.1 (C2″), 130.6 (C8), 130.8 (C9a), 132.4 (C9), 137.4 (C8a′), 141.6 (C3a), 154.9 (C5), 156.8 (C4″), 161.3 (C═O), 165.7 (NHC(O)).

*DUBA (**3b**).* *seco*-DUBA (0.27 g, 0.51 mmol) was dissolved in DMA (4 mL). Water (2 mL) and $NaHCO_3$ (85 mg, 1.01 mmol) were added, and the mixture was stirred for 17 h. The reaction mixture was then diluted with water and filtered. The residue was suspended in toluene, and the suspension was concentrated to dryness to give DUBA (**3b**, 143 mg, 57%).

^{1}H NMR (DMSO-d_6, 400 MHz): δ = 1.36 (1H, m, H9), 2.14 (1H, m, H9), 2.42 (3H, 8-CH_3), 3.75 (1H, m, H9a), 4.61 (1H, dd, H1), 4.90 (1H, d, H1), 6.89 (2H, d, H3″), 7.18 (1H, s, H3), 7.33 (1H, t, H6), 7.39 (1H, d, H7), 7.60 (1H, dd, H8′), 7.72 (1H, d, H7′), 7.90 (2H, d, H2″), 8.04 (1H, d, H5), 8.68 (1H, s, H3′), 9.46 (1H, s, H5′), 10.21 (1H, s, NH). ^{13}C NMR (DMSO-d_6, 100 MHz): δ = 20.3 (8-CH_3), 22.5 (C9), 24.6 (C9a), 33.1 (C8b), 54.9 (C1), 109.9 (C3), 115.5 (C3″), 117.4 (C5′), 118.0 (C7′), 120.2 (C3′), 123.9 (C8′), 125.0 (C5), 126.5 (C6), 128.2 (C6′), 130.2 (C2″), 133.8 (C4a), 133.8 (C8a), 134.1 (C1″), 135.8 (C7), 138.2 (C8), 140.0 (C2′), 141.8 (C8a′), 161.3 (C4″), 162.8 (C2a), 164.0 (C═O), 165.8 (NHC(O)), 185.3 (C4).

*Compound **26**.* The synthesis of compound **26** was carried out analogously to that of **3a**, starting from compound **15**, compound **20**, and ethyl 5-amino-1*H*-indole-2-carboxylate.[30] Compound **26** was obtained from **15** in 75% overall yield.

^{1}H NMR (DMSO-d_6, 400 MHz): δ = 2.81 (3H, s, 9-CH_3), 3.53 (1H, dd, CH_2Cl), 3.82 (1H, d, CH_2Cl), 4.34 (1H, t, H1), 4.59 (1H, d, H2), 4.71 (1H, dd, H2), 6.91 (2H, d, H3″), 7.19 (1H, d, H3′), 7.27 (1H, dd, H7), 7.36 (1H, d, H8), 7.47 (1H, d, H4′), 7.57 (1H, dd, H6′), 7.90 (2H, d, H2″), 8.03 (1H, s, H4), 8.07 (1H, d, H6), 8.17 (1H, d, H7′), 9.96 (1H, s, OH), 10.07 (1H, s, NHC(O)), 10.49 (1H, s, OH), 11.7 (1H, s, NH). ^{13}C NMR (DMSO-d_6, 100 MHz): δ = 22.9, 44.7, 48.0, 55.1, 100.6, 106.0, 112.4, 113.4, 115.3, 115.6, 120.1, 122.0, 123.3, 123.8, 126.2, 127.4, 130.0, 130.5, 130.8, 131.7, 132.6, 132.7, 133.7, 143.0, 155.1, 160.7, 160.8, 165.3.

*1-(2-(2-Hydroxyethoxy)ethyl)-1H-pyrrole-2,5-dione (**33**).* A saturated solution of $NaHCO_3$ in water (500 mL) was cooled to 0 °C, after which 2-(2-aminoethoxy)ethanol (**32**, 9.68 mL, 96.5 mmol) was added. The mixture was stirred for 20 min at 0 °C. Then, **31** (15 g, 97 mmol) was added as a powder, and the resulting mixture was stirred for 50 min, slowly being warmed to room temperature. The mixture was extracted with CH_2Cl_2, and the combined organic layers were dried with $MgSO_4$, filtered, and concentrated to yield **33** as a colorless oil (13 g, 73%).

^{1}H NMR ($CDCl_3$, 400 MHz): δ = 2.53 (1H, t, OH), 3.56−3.58 (2H, m, CH_2OH), 3.64−3.71 (4H, m, CH_2OCH_2), 3.73−3.76 (2H, m, NCH_2), 6.73 (2H, s, CH═CH). ^{13}C NMR ($CDCl_3$, 100 MHz): δ = 37.2 (NCH_2), 67.4 (CH_2OCH_2), 67.9 (CH_2OCH_2), 68.5 (CH_2OH), 135.0 (CH═CH), 170.8 (C═O).

*2-(2-(2,5-Dioxo-2,5-dihydro-1H-pyrrol-1-yl)ethoxy)ethyl (4-Nitrophenyl) Carbonate (**34**).* To a solution of **33** (11.6 g, 62.9 mmol) in CH_2Cl_2 (350 mL) at 0 °C under a nitrogen atmosphere were added Et_3N (30.6 mL, 220 mmol) and 4-nitrophenyl chloroformate (15.2 g, 75.5 mmol). The mixture was stirred at room temperature for 2.5 h. After addition of CH_2Cl_2 (150 mL), the mixture was washed with a saturated aqueous $NaHCO_3$ solution and water, dried with Na_2SO_4, and concentrated. The crude product was purified using column chromatography (CH_2Cl_2/EtOAc, 1:0 to 4:1, v/v) to yield **34** (20.9 g, 95%) as a white solid.

^{1}H NMR (DMSO-d_6, 400 MHz): δ = 3.62 (4H, m, NCH_2CH_2), 3.71 (2H, m, OCH_2), 4.35 (2H, m, CH_2OC(O)), 7.04 (2H, s, CH═CH), 7.58 (2H, m, H2′), 8.34 (2H, m, H3′). ^{13}C NMR (DMSO-d_6, 100 MHz): δ = 37.2 (NCH_2), 67.4 (CH_2OCH_2), 67.9 (CH_2OCH_2), 68.5 (CH_2OC(O)), 123.0 (C2′), 125.9 (C3′), 135.0 (CH═CH), 145.6 (C1′), 152.5 (OC(O)NH), 155.7 (C4′), 171.4 (OC(O)O).

*Compound **36**.* To a solution of **34** (3.0 g, 8.6 mmol) in anhydrous DMF (30 mL) at 0 °C were added **35** (3.25 g, 8.56 mmol) and *i*-Pr_2NEt (3.74 mL, 21.4 mmol). The resulting mixture was stirred for 2 h and then concentrated. The crude product was purified by column chromatography (CH_2Cl_2/methanol, 1:0 to 2:1, v/v) to yield **36** as a white solid in quantitative yield.

^{1}H NMR (DMSO-d_6, 400 MHz): δ = 0.84 (3H, d, $CH_{3,Val}$), 0.88 (3H, d, $CH_{3,Val}$), 1.36−1.48 (2H, m, β-H_{Cit}), 1.58−1.75 (2H, m, γ-H_{Cit}), 1.99 (1H, m, β-H_{Val}), 2.94−3.07 (2H, m, CH_2NH_{Cit}), 3.53−3.61 (6H, m, $CH_2CH_2OCH_2$), 3.91 (1H, m, α-H_{Val}), 4.00−4.07 (2H, m, CH_2OC(O)), 4.38−4.45 (3H, m, α-H_{Cit}, CH_2OH), 5.11 (1H, t, OH), 5.43 (2H, s, NH_2), 6.01 (1H, t, NH_{Cit}), 7.04 (2H, s, CH═CH), 7.19−7.26 (3H, m, NH_{Val}, C3′), 7.55 (2H, d, C2′), 8.08 (1H, d, NH_{Cit}), 9.98 (1H, s, NH_{PABA}). ^{13}C NMR (DMSO-d_6, 100 MHz): δ = 18.6 ($CH_{3,Val}$), 19.7 ($CH_{3,Val}$), 27.2 (β-$CH_{2,Cit}$), 30.0 (γ-$CH_{2,Cit}$), 30.9 (β-CH_{Val}), 37.2 (NCH_2), 39.1 (CH_2NH_{Cit}), 53.5 (α-CH_{Cit}), 60.5 (α-CH_{Val}), 63.1 (CH_2OH), 63.8 (CH_2OC(O)), 67.4 (CH_2OCH_2), 68.8 (CH_2OCH_2), 119.3 (C2′), 127.4 (C3′), 135.0 (CH═CH), 137.9 (C4′), 138.0 (C1′), 156.6 (OC(O)NH), 159.4 (C(O)NH_2), 170.9 (C═O_{Cit}), 171.4 (C═$O_{maleimide}$), 171.7 (C═O_{Val}).

*Compound **37**.* To solution of **36** (5.1 g, 8.6 mmol) in anhydrous DMF (30 mL) at 0 °C were added bis(4-nitrophenyl) carbonate (5.21 g, 17.1 mmol) and *i*-Pr_2NEt (2.24 mL, 12.8 mmol). The resulting mixture was stirred for 2 h and then concentrated. The crude product was purified by column chromatography (CH_2Cl_2/methanol, 1:0 to 9:1, v/v), fractions containing product were pooled and concentrated, and the product was lyophilized from 1,4-dioxane/water to yield **37** (4.9 g, 77%) as a white solid.

^{1}H NMR (DMSO-d_6, 400 MHz): δ = 0.86 (3H, d, $CH_{3,Val}$), 0.90 (3H, d, $CH_{3,Val}$), 1.38−1.50 (2H, m, β-H_{Cit}), 1.62−1.74 (2H, m, γ-H_{Cit}), 2.00 (1H, m, β-H_{Val}), 2.95−3.09 (2H, m, CH_2NH_{Cit}), 3.53−3.72 (6H, m, $CH_2CH_2OCH_2$), 3.92 (1H, m, α-H_{Val}), 4.02−4.06 (2H, m, CH_2OC(O)NH), 4.46 (1H, m, α-

DOI: 10.1021/mp500781a
Mol. Pharmaceutics 2015, 12, 1813−1835

H_{Cit}), 5.27 (2H, s, $CH_2OC(O)O$), 5.45 (2H, s, NH_2), 6.00 (1H, t, NH_{Cit}), 7.04 (2H, s, CH=CH), 7.20 (1H, d, NH_{Val}), 7.43 (2H, d, H3′), 7.58 (2H, m, H2″), 7.67 (2H, d, H2′), 8.11−8.14 (1H, m, NH_{Cit}), 8.34 (2H, m, H3″), 10.14 (1H, s, NH_{PABA}). ^{13}C NMR (DMSO-d_6, 100 MHz): δ = 18.6 ($CH_{3,Val}$), 19.7 ($CH_{3,Val}$), 27.3 (β-$CH_{2,Cit}$), 29.9 (γ-$CH_{2,Cit}$), 30.9 (β-CH_{Val}), 37.2 (NCH_2CH_2), 39.1 (CH_2NH), 53.6 (α-CH_{Cit}), 60.5 (α-CH_{Val}), 63.8 ($CH_2OC(O)NH$), 67.4 (CH_2OCH_2), 68.8 (CH_2OCH_2), 70.7 ($CH_2OC(O)O$), 119.5 (C2′), 123.1 (C2″), 125.9 (C3″), 129.8 (C4′), 130.0 (C3′), 135.0 (CH=CH), 139.9 (C1′), 145.7 (C1″), 152.5 (OC(O)O), 155.8 (C4″), 156.6 (OC(O)NH), 159.4 ($C(O)NH_2$), 171.2 (C=O_{Cit}), 171.4 (C=$O_{maleimide}$), 171.8 (C=O_{Val}).

Compound ***39***. A solution of **25** (100 mg, 0.175 mmol) in anhydrous THF (10 mL) was cooled to 0 °C under a nitrogen atmosphere, after which 4-nitrophenyl chloroformate (46 mg, 0.23 mmol) and Et_3N (0.12 mL, 0.88 mmol) were added. The mixture was stirred at 0 °C for 1.5 h. Then, **38** (165 mg, 0.875 mmol) was added, and the mixture was stirred for another 1 h, slowly being warmed to room temperature. The reaction mixture was then concentrated, and the crude product was purified by column chromatography (CH_2Cl_2/methanol, 1:0 to 97:3, v/v) to yield **39** as a yellow solid (128 mg, 93%).

^{1}H NMR (DMSO-d_6, 400 MHz): δ = 1.40 (9H, m, Boc), 2.74−3.03 + 3.23 (6H, multiple s, 2 × NCH_3), 2.83 (3H, s, 9-CH_3), 3.23−3.54 (4H, m, NCH_2CH_2), 3.41 (3H, s, OCH_3), 3.71 (1H, m, CH_2Cl), 3.82 (1H, d, CH_2Cl), 4.44 (1H, t, H1), 4.66 (1H, m, H2), 5.18 (1H, d, H2), 5.30 (2H, s, OCH_2O), 7.17 (2H, d, H3″), 7.32 (1H, m, H7), 7.40 (1H, m, H8), 7.58 (1H, m, H8′), 7.66−7.81 (2H, m, H6, H7′), 7.99 (2H, d, H2″), 8.37 (1H, br s, H4), 8.69 (1H, s, H3′), 9.45 (1H, s, H5′), 10.30 (1H, s, NH). ^{13}C NMR (DMSO-d_6, 100 MHz): δ = 22.4 (9-CH_3), 28.0 + 28.1 + 28.4 ($CH_{3,Boc}$), 33.8 + 34.0 + 34.6 + 34.7 + 34.9 (NCH_3), 44.3 (C1), 45.1 + 45.7 + 45.8 + 46.4 + 46.5 + 46.7 (NCH_2), 47.5 (CH_2Cl), 54.6 (C2), 55.8 (OCH_3), 78.7 (C_{Boc}), 78.8 (C_{Boc}), 93.7 (OCH_2), 110.7 (C4), 115.7 (C3″), 117.3 (C5′), 117.6 (C7′), 119.1 (C3′), 120.8 (C6), 122.3 (C9b), 123.1 (C8′), 124.9 (C7), 125.7 + 125.9 (C5a), 127.3 (C1″), 127.5 (C2′), 129.6 (C2″), 129.8 (C9a), 130.6 (C8), 132.9 (C9), 140.6 (C6′), 141.4 (C8a′), 141.9 (C3a), 148.0 + 148.2 (C=O), 153.9 + 153.9 (C5), 154.8 + 154.8 + 155.1 (C=O_{Boc}), 159.6 (C4″), 161.9 (C=O), 165.1 (NHC(O)).

Linker-Drug ***29***. A solution of **39** (128 mg, 0.163 mmol) in CH_2Cl_2 (6 mL) was cooled to 0 °C, after which TFA (6 mL) was added. The mixture was stirred at 0 °C for 1 h, diluted with CH_2Cl_2 (20 mL), and concentrated. The residue was dissolved in CH_2Cl_2/toluene, and the mixture was concentrated to yield crude **40**, which was used in the next step without further purification.

Compound **40** was dissolved in anhydrous DMF (4 mL), and the solution was cooled to 0 °C under a nitrogen atmosphere, after which **37** (135 mg, 0.179 mmol) was added, followed by Et_3N (0.11 mL, 0.82 mmol). The mixture was stirred for 2 h, gradually being warmed to room temperature, and then concentrated. The crude linker-drug was then purified by column chromatography (CH_2Cl_2/methanol, 1:0 to 17:3, v/v) and preparative HPLC (acetonitrile/0.1% TFA in water, 3:7 to 6:4, v/v). The fractions containing product were pooled, acetonitrile was evaporated, and the resulting aqueous suspension was freeze-dried. The resulting powder was redissolved in 1,4-dioxane/water, and the solution was freeze-dried to yield **29** (110 mg, 49%) as its TFA salt.

^{1}H NMR (DMSO-d_6, 400 MHz): δ = 0.83 (3H, d, $CH_{3,Val}$), 0.87 (3H, d, $CH_{3,Val}$), 1.32−1.50 (2H, m, β-H_{Cit}), 1.52−1.73 (2H, m, γ-H_{Cit}), 1.97 (1H, m, β-H_{Val}), 2.83 (3H, s, 9-CH_3), 2.84−3.24 (8H, m, CH_2NH_{Cit}, 2 × NCH_3), 3.43−3.62 (10H, m, 2 × CH_2NCH_3, $CH_2CH_2OCH_2$), 3.74 (1H, m, CH_2Cl), 3.82 (1H, d, CH_2Cl), 3.91 (1H, m, α-H_{Val}), 3.98−4.05 (2H, m, $CH_2OC(O)NH$), 4.58 (2H, br s, NH_2), 4.40−4.47 (2H, m, H1, α-H_{Cit}), 4.66 (1H, m, H2), 4.94−5.10 (3H, m, H2, Ar−$CH_2OC(O)$), 6.06 (1H, t, NH_{cit}), 6.91 (2H, d, H3″), 7.00 (2H, s, CH=CH), 7.16−7.41 (5H, m, H7, H8, H3‴, NH_{Val}), 7.47−7.61 (2H, m, H2‴), 7.62−7.80 (3H, m, H6, H7′, H8′), 7.92 (2H, d, H2″), 8.10 (1H, m, NH_{Cit}), 8.32 (1H, br s, H4), 8.85 (1H, br s, H3′), 9.59 (1H, d, H5′), 9.98−10.05 (2H, m, OH, NH_{PABA}), 10.33 (1H, s, 6′-NHC(O)). ^{13}C NMR (DMSO-d_6, 100 MHz): 18.2 ($CH_{3,Val}$), 19.2 ($CH_{3,Val}$), 22.4 (9-CH_3), 26.8 (β-$CH_{2,Cit}$), 29.5 (γ-$CH_{2,Cit}$), 30.5 (β-CH_{Val}), 33.8 + 34.3 + 34.5 + 34.6 + 34.8 + 34.9 (2 × NCH_3), 36.7 (CH_2NCH_3), 38.7 (CH_2NH), 44.4 (C1), 45.6 + 45.9 + 46.3 + 46.6 (CH_3NCH_2), 47.51 (CH_2Cl), 53.2 (α-CH_{Cit}), 54.4 (C2), 60.1 (α-CH_{Val}), 63.4 ($CH_2OC(O)NH$), 66.1 + 66.3 + 66.4 (Ar−$CH_2OC(O)$), 67.0 (CH_2OCH_2), 68.4 (CH_2OCH_2), 110.4 + 110.6 (C4), 115.2 (C3″), 115.8 (C7′), 117.5 (C5′), 118.6 (C3′), 119.0 (C2‴), 120.7 (C6), 122.7 (C9b), 124.4 (C1″), 125.0 (C5a), 125.6 (C7), 126.0 (C8′), 128.4 + 128.6 + 128.7 (C3‴), 128.8 (C2′), 129.8 (C9a), 129.9 (C2″), 130.7 (C8), 131.6 + 131.7 + 131.8 (C4‴), 133.1 (C9), 134.6 (CH=CH), 138.6 (C1‴), 138.7 (C6′), 139.9 (C8a′), 141.5 (C3a), 148.1 + 148.2 (5-OC(O)), 153.8 + 154.1 (C5), 155.5 + 155.6 + 155.9 (Ar−$CH_2OC(O)$), 156.2 (OC(O)NH), 158.4 (q, C=O_{TFA}), 159.0 ($C(O)NH_2$), 160.0 (3-C(O)), 161.1 (C4″), 165.5 (6′-NHC(O)), 170.6 (C=O_{Cit}), 170.9 (C=$O_{maleimide}$), 171.3 (C=O_{Val}).

Compound ***41***. A solution of **25** (100 mg, 0.175 mmol) in anhydrous THF (10 mL) was cooled to 0 °C under a nitrogen atmosphere, after which 4-nitrophenyl chloroformate (46 mg, 0.23 mmol) and Et_3N (0.12 mL, 0.88 mmol) were added. The mixture was stirred at 0 °C for 1.5 h, *N*-methylpiperazine (0.10 mL, 0.88 mmol) was added, and the mixture was stirred for another hour, gradually being warmed to room temperature. The reaction mixture was then concentrated, and the crude product was purified by column chromatography (CH_2Cl_2/methanol, 1:0 to 9:1, v/v), yielding **41** as a yellow glassy solid (98 mg, 80%).

^{1}H NMR ($CDCl_3$, 400 MHz): δ = 2.45 (3H, s, NCH_3), 2.63 (4H, m, 2 × CH_2NCH_3), 2.75 (3H, s, 9-CH_3), 3.15 (1H, t, CH_2Cl), 3.51 (1H, dd, CH_2Cl), 3.53 (3H, s, OCH_3), 3.77 (2H, m, $CH_2NC(O)$), 3.93 (2H, m, $CH_2NC(O)$), 4.18 (1H, t, H1), 4.33 (1H, dd, H2), 5.20 (2H, s, OCH_2O), 5.41 (1H, d, H2), 6.79 (2H, d, H-3″), 7.01 (1H, t, H7), 7.08 (1H, d, H8), 7.27 (1H, d, H8′), 7.38 (2H, d, H2″), 7.50 (1H, d, H7′), 7.52 (1H, d, H6), 8.06 (1H, s, H4), 8.45 (1H, s, NH), 8.51 (1H, s, H3′), 9.09 (1H, s, H5′). ^{13}C NMR ($CDCl_3$, 100 MHz): δ = 22.9 (9-CH_3), 44.4 ($CH_2NC(O)$), 44.9 ($CH_2NC(O)$), 45.7 (NCH_3), 46.4 (C1), 46.7 (CH_2Cl), 54.5 (CH_2NCH_3), 54.9 (CH_2NCH_3), 55.0 (C2), 56.4 (OCH_3), 94.3 (OCH_2O), 111.5 (C3′), 115.4 (C3″), 115.8 (C5′), 118.4 (C7′), 119.2 (C4), 120.4 (C6), 122.0 (C8′), 122.8 (C9b), 124.7 (C7), 126.0 (C5a), 126.8 (C1″), 127.7 (C2′), 129.0 (C2″), 130.1 (C9a), 130.7 (C8), 132.8 (C9), 140.6 (C6′), 141.9 (C8a′), 142.1 (C3a), 147.9 (5-OC(O)), 154.4 (C5), 159.8 (C4″), 162.3 (3-C(O)), 165.2 (6′-NHC(O)).

Compound ***43***. A solution of **41** (98 mg, 0.14 mmol) in CH_2Cl_2 (6 mL) was cooled to 0 °C, after which TFA (6 mL)

DOI: 10.1021/mp500781a
Mol. Pharmaceutics 2015, 12, 1813−1835

was added. The mixture was stirred at 0 °C for 1.5 h, then diluted with CH_2Cl_2 (20 mL), and concentrated. The residue was dissolved in CH_2Cl_2/toluene, and the mixture was concentrated. The crude product was purified by column chromatography (CH_2Cl_2/methanol, 1:0 to 8:2, v/v) to yield **42** as a yellow glassy solid. The intermediate was dissolved in anhydrous THF (10 mL), and the solution was cooled to 0 °C under a nitrogen atmosphere. 4-Nitrophenyl chloroformate (37 mg, 0.18 mmol) and Et_3N (90 μL, 0.71 mmol) were added. The mixture was stirred at 0 °C for 3 h, **38** (132 mg, 0.705 mmol) was added, and the mixture was stirred for another hour, slowly being warmed to room temperature. The mixture was concentrated, and the crude product was purified by column chromatography (CH_2Cl_2/methanol, 1:0 to 9:1, v/v) to yield **43** as a yellow solid (47 mg, 38%).

^{1}H NMR (DMSO-d_6, 400 MHz): δ = 1.33 + 1.39 (9H, 2 × s, Boc), 2.30 (3H, s, $CH_2N(CH_3)CH_2$), 2.24−2.36 + 2.44−2.56 (4H, 2 × m, $CH_2N(CH_3)CH_2$), 2.80 (3H, s, 9-CH_3), 2.80−3.00 (6H, multiple s, 2 × $N(CH_3)C(O)$), 3.41 (2H, m, $CH_2N(CH_3)C(O)$), 3.35−3.57 (5H, m, $CH_2N(CH_3)C(O)$, CH_2Cl, $CH_2N(C(O))CH_2$), 3.77−3.84 (3H, m, CH_2Cl, $CH_2N(C(O))CH_2$), 4.42 (1H, t, H1), 4.64 (1H, t, H2), 5.16 (1H, d, H2), 7.24 (2H, d, H3″), 7.33 (1H, dd, H7), 7.38 (1H, t, H8), 7.63 (1H, t, H8′), 7.69−7.73 (2H, m, H6, H7′), 8.06 (2H, d, H2″), 8.33 (1H, br s, H4), 8.66 (1H, s, H3′), 9.45 (1H, s, H5′), 10.05 (1H, s, NH). ^{13}C NMR (DMSO-d_6, 100 MHz): δ = 22.3 (9-CH_3), 28.0 ($CH_{3,Boc}$), 33.8 ($N(CH_3)C(O)$), 34.7 ($N(CH_3)C(O)$), 43.3 ($CH_2N(CH_3)C(O)$), 43.9 (CH_2N-$(CH_3)C(O)$), 44.2 (C1), 45.2 ($CH_2N(CH3)CH_2$), 46.1 ($CH_2N(C(O))CH_2$), 46.5 ($CH_2N(C(O))CH_2$), 47.4 (CH_2Cl), 53.8 ($CH_2N(CH_3)CH_2$), 54.1 ($CH_2N(CH_3)CH_2$), 54.5 (C2), 110.6 (C4), 117.3 (C5′), 117.4 (C7′), 119.1 (C3′), 120.5 (C6), 121.1 (C3″), 122.3 (C9b), 123.0 (H8′), 124.7 (C7), 125.6 (C5a), 127.4 (C1″), 129.1 (C2″), 129.7 (C2′), 130.5 (C8), 130.9 (C9a), 133.0 (C9), 140.5 (C6′), 141.4 (C8a′), 141.8 (C3a), 147.7 (5-OC(O)), 152.6 (C5), 153.4 ($OC(O)N(CH_3)CH_2$), 153.9 ($OC(O)N(CH_3)CH_2$), 161.8 (3-C(O)), 164.9 (6′-NHC(O)).

Linker-Drug ***30***. A solution of **43** (47 mg, 0.054 mmol) in CH_2Cl_2 (3 mL) was cooled to 0 °C, after which TFA (3 mL) was added. The mixture was stirred at 0 °C for 40 min, then diluted with CH_2Cl_2 (20 mL) and concentrated to dryness to yield crude **44** as its TFA salt. The crude intermediate was dissolved in anhydrous DMF (2 mL). The solution was cooled to 0 °C, after which **37** (135 mg, 0.179 mmol) and Et_3N (0.11 mL, 0.81 mmol) were added. The mixture was stirred for 2 h and gradually warmed to room temperature. The mixture was then concentrated, and the crude product was purified by column chromatography (CH_2Cl_2/methanol, 1:0 to 3:1, v/v) to yield partly purified **30** (55 mg) as a yellow solid. Further purification was carried out by preparative HPLC (acetonitrile/0.1% TFA in water, 3:7 to 6:4, v/v). The fractions containing product were pooled, acetonitrile was evaporated, and the resulting aqueous suspension was freeze-dried. The resulting powder was redissolved in 1,4-dioxane/water, and the solution was freeze-dried to yield **30** (41 mg, 47%) as its TFA salt.

^{1}H NMR (DMSO-d_6, 400 MHz): δ = 0.81 (3H, d, $CH_{3,Val}$), 0.85 (3H, d, $CH_{3,Val}$), 1.36−1.46 (2H, m, β-H_{Cit}), 1.58−1.68 (2H, m, γ-H_{Cit}), 1.95 (1H, m, β-H_{Val}), 2.85 (3H, s, 9-CH_3), 2.86−3.05 (11H, m, CH_2NH_{Cit}, 3 × NCH_3), 3.18−3.62 (19H, m, CH_2Cl, $CH_2CH_2OCH_2$, $CH_2N(CH_3)CH_2$, 2 × CH_2N-$(CH_3)C(O)$, $CH_2N(C(O))CH_2$), 3.84−3.90 (2H, m, CH_2Cl, α-CH_{Val}), 3.96−4.01 (2H, m, $CH_2OC(O)NH$), 4.12−4.74 (5H, m, H1, H2, α-CH_{Cit}, NH_2), 4.97−5.08 (3H, m, H2, Ar−$CH_2OC(O)$), 6.07 (1H, br s, NH_{cit}), 7.04 (2H, s, CH=CH), 7.19 (1H, m, NH_{Val}), 7.22−7.34 (4H, m, H3″, H3‴), 7.37−7.40 (1H, m, H7), 7.45 (1H, m, H8), 7.56−7.64 (2H, m, H2‴), 7.71 (1H, m, H8′), 7.79−7.83 (2H, m, H6, H7′), 8.01−8.05 (2H, m, H2″), 8.09 (1H, d, NH_{Cit}), 8.40 (1H, s, H4), 8.83 (1H, s, H3′), 9.58 (1H, s, H5′), 10.05 (1H, s, NH_{PABA}), 10.57 (1H, s, 6′-NHC(O)). ^{13}C NMR (DMSO-d_6, 100 MHz): δ = 18.1 ($CH_{3,Val}$), 19.2 ($CH_{3,Val}$), 22.4 (9-CH_3), 26.8 (β-$CH_{2,Cit}$), 29.4 (γ-$CH_{2,Cit}$), 30.4 (β-CH_{Val}), 33.9 + 34.4 + 34.6 + 34.6 + 34.8 + 34.9 (2 × $N(CH_3)C(O)$), 36.7 ($CH_2CH_2OCH_2$), 38.7 (CH_2NH), 42.3 ($CH_2N(CH_3)CH_2$), 44.3 (C1), 45.4 + 45.8 + 46.0 + 46.4 + 46.5 + 46.7 (2 × $CH_2N(CH_3)C(O)$, $CH_2N(C(O))CH_2$), 47.6 (CH_2Cl), 52.1 ($CH_2N(CH_3)CH_2$), 53.1 (α-CH_{Cit}), 54.6 (C2), 60.1 (α-CH_{Val}), 63.3 ($CH_2OC(O)$-NH), 66.1 + 66.3 (Ar−$CH_2OC(O)$), 66.9 (CH_2OCH_2), 68.4 (CH_2OCH_2), 110.6 (C4), 116.6 (C7′), 117.7 (C5′), 119.0 (C3′, C2‴), 120.7 (C6), 121.7 + 121.8 + 121.9 (C3″), 122.9 (C9b), 124.2 (C1″), 124.6 (C8′), 125.0 (C7), 125.7 (C5a), 128.1 (C9a), 128.4 + 128.6 (C3‴), 129.2 (C2″), 129.8 (C9a), 130.8 (C8), 130.9 (C2′), 131.5 + 131.6 + 131.7 + 131.8 (C4‴), 133.2 (C9), 134.6 (CH=CH), 138.1 (C1‴), 138.7 (C6′), 139.9 (C8a′), 141.5 (C3a), 147.6 (5-$OC(O)$), 152.4 (C5), 153.4 + 153.5 + 153.7 (Ar−$CH_2OC(O)$), 155.5, 155.6, 155.8 (4″-$OC(O)$), 156.2 ($OC(O)NH$), 158.4 (q, $C=O_{TFA}$), 159.0 ($C(O)NH_2$), 160.8 (3-C(O)), 165.2 (6′-NHC(O)), 170.6 ($C=O_{Cit}$), 170.9 ($C=O_{maleimide}$), 171.3 ($C=O_{Val}$).

LogD Determination of *seco*-DUBA. The distribution coefficient at pH 7.4 ($logD_{7.4}$) was determined by UPLC-UV using a system calibration with a set of seven reference compounds.[63,64] The respective retention times of the reference compounds were plotted versus the literature $logD_{7.4}$ values, and linear regression was performed. The $logD_{7.4}$ value of *seco*-DUBA was estimated by interpolating its retention time on the linear calibration curve. Analysis was carried out with an Acquity BEH Shield RP18 column (Waters) using a 4 min gradient of 5 to 95% mobile phase B (100% acetonitrile) in mobile phase A (10 mM ammonium acetate, pH 7.4) at a flow rate of 0.5 mL/min.

In Vitro Cytotoxicity of ADCs. Human tumor cell lines obtained from ATCC were cultured as described previously.[43] Cells in complete growth medium were plated in 96-well plates (90 μL/well) and incubated at 37 °C, 5% CO_2 at the following cell densities (cells per well): 6500 for SK-BR-3, 10,000 for BT-474c, 2000 for SK-OV-3, and 4000 for SW620. After overnight incubation, 10 μL of a test compound solution was added. When plasma stability was assessed, 1% human or mouse plasma was present in the complete growth medium used for cell addition and compound addition. Cell viability in serial dilutions was assessed after 144 h using the CellTiter-Glo luminescent assay kit from Promega Corporation (Madison, WI, USA) according to the manufacturer's instructions. Metabolic activity of BT-474c cells was measured with an ATP-Lite assay (PerkinElmer, Waltham, MA, USA). Data were reported as mean ± SEM of at least two experiments performed in duplicate.

Human Plasma Stability of HSA-Conjugated Linker-Drugs 29 and 30. A stock solution of linker-drug (12.5 μL, 300 μM in DMSO) was added to human plasma (487.5 μL) at 37 °C, which led to almost instantaneous addition of the linker-drug to HSA. At defined time points, aliquots (50 μL) were taken and added to cold acetonitrile (200 μL). The resultant

DOI: 10.1021/mp500781a
Mol. Pharmaceutics 2015, 12, 1813−1835

suspension was spun down, and the supernatant was analyzed for DUBA and **27** by UPLC-MS using single ion recording.

Determination of the Cyclization Rate of Compounds 47a and 47b. Compounds **47a** and **47b** were obtained from their protected counterparts using a similar procedure as described for compound **39**, except that HCl instead of TFA was used for deprotection. The crude HCl salt of **47a** or **47b** was dissolved in DMSO at 1 mg/mL, and 3 μL of this solution was added to a preheated vial containing either acetonitrile/10 mM NaOAc, pH 5 (2:3, v/v), or acetonitrile/100 mM Na_3PO_4, pH 7.4 (2:3, v/v). After thorough mixing, the mixtures were placed in an autosampler at 25 or 37 °C. Samples were taken at different time intervals and directly injected onto a UPLC column to measure the decrease of **47a** and **47b** over time. Half-lives were calculated from the UV peak areas of **47a** and **47b**.

Plasma Stability Studies with ADCs and DUBA. ADCs SYD981, SYD982, SYD983, and SYD984 were spiked in pooled female mouse (Balb/c), rat (Sprague−Dawley), cynomolgus monkey (*Macaca fascicularis*), and human K2-EDTA plasma at a concentration of 100 μg/mL and incubated at 37 °C. After 0, 1, 6, 24, 48, 96, and 168 h of incubation, plasma samples were snap-frozen and stored at −80 °C until analysis. DUBA was spiked in pooled female mouse (Balb/c), rat (Sprague−Dawley), cynomolgus monkey (*M. fascicularis*), and human K2-EDTA plasma at a concentration of 5 nM and incubated at 37 °C. After 0, 3, 10, 30, 90, and 180 min of incubation, plasma samples were stored at −80 °C until analysis by LC-MS/MS. On the basis of the time−concentration data, the in vitro plasma half-life ($t_{1/2}$) was calculated using the expression $t_{1/2} = 0.693/b$, where b is the slope found in the linear fit of the natural logarithm of the fraction remaining of total antibody or ADC versus incubation time. Only the initial, linear part of this fit was used to determine the $t_{1/2}$. If a calculated $t_{1/2}$ was more than 2-fold the longest incubation time of 168 h, the $t_{1/2}$ was reported as >336 h.

PK ELISA. *Total Antibody Assay.* An ELISA-based method was used for the determination of total antibody concentrations for SYD981, SYD982, SYD983, and SYD984. Study samples were diluted in appropriate buffers in order to be able to estimate the total antibody concentrations within the analytical range. The solid phase consisted of an anti-idiotype mini-antibody (AbD Serotec, AbD15916) coated on high binding microtiter plates (Greiner, catalog no. 655081). Detection of total antibody captured on the solid phase was achieved by a biotinylated anti-idiotype mini-antibody, followed by a streptavidin-HRP (R&D Systems, catalog no. DY998) incubation step and TMB (TeBu-Bio, catalog no. TMB100) incubation. The color reaction was stopped with H_2SO_4, and the plate was read at 450 and 630 nm. Each analytical run included appropriate calibrators and quality-control samples. Total antibody concentrations of study samples were back calculated on the calibrator curve.

Conjugated Antibody Assay. A similar method as for the total antibody assay was used with the exception that the solid phase consisted of an antidrug monoclonal antibody (Synthon Biopharmaceuticals BV, clone B 6−2−10) coated on high binding microtiter plates (Greiner, catalog no. 655081).

In Vivo Pharmacokinetics in Mice, Rats, and Monkeys. ADCs SYD981, SYD982, SYD983, and SYD984 were dosed to female Balb/c mice, female Sprague−Dawley rats, and female cynomolgus monkeys via an intravenous bolus injection into the tail vein or saphenous vein. DUBA and *seco*-DUBA were dosed to female Wistar Han rats via an intravenous bolus injection into the tail vein. Blood samples were taken from an appropriate (different) vein at different time points after dosing, cooled on ice water, and processed to K2-EDTA plasma. Plasma samples where snap-frozen in liquid nitrogen and stored at −80 °C until bioanalysis. On the basis of the reported plasma levels, PK parameters were calculated in WinNonlin version 5.1.5 or 5.3 using the noncompartmental analysis for single intravenous bolus injection. Two ELISA-based methods were used for quantification of either total antibody or conjugated antibody. A validated LC-MS/MS method was used for the quantification of DUBA plasma levels.

■ ASSOCIATED CONTENT

Ⓢ Supporting Information

Table with confidence intervals and efficacy percentages, complementing the in vitro IC_{50} data, table with AUC data from PK studies, and NMR spectra for some key intermediates, drugs, and linker-drugs. This material is available free of charge via the Internet at http://pubs.acs.org.

■ AUTHOR INFORMATION

Corresponding Author

*E-mail: patrick.beusker@synthon.com. Phone: +31 24 372 77 00. Fax: +31 24 372 77 05.

Notes

The authors declare the following competing financial interest(s): Dr. J. M. Lemmens owns stock in Synthon BV.

■ ACKNOWLEDGMENTS

We thank our Synthon colleagues J. Eigenhuijsen, E. Mattaar, J. Verhagen, C. Oppers-Tiemissen, and R. Martens for performing several bioanalytical assays, T. van Achterberg and E. Loosveld for carrying out some in vitro assays, M. van der Vleuten for managing the in vivo studies, P. Renart Verkerk for performing several conjugation reactions, R. Buurman for development of the logD assay and sample analysis, G. de Roo and R. Verstegen for development of the HIC purification step, M. Káš, V. Janoušek, I. Bláha, and J. Píš for optimization of some synthetic steps, and V. de Matteis and L. van den Broek for critical review of the manuscript.

■ ABBREVIATIONS

Ac, acetyl; ADC, antibody−drug conjugate; AUC, area under the curve; Bn, benzyl; Boc, *tert*-butoxycarbonyl; Bu, butyl; *t*-Bu, *tert*-butyl; CES1c, carboxylesterase 1c; DAR, drug-to-antibody ratio; DMA, *N*,*N*-dimethylacetamide; DMF, *N*,*N*-dimethylformamide; DPPA, diphenylphosphoryl azide; DUBA, duocarmycin-hydroxybenzamide-azaindole; EDC, 1-ethyl-3-(3-(dimethylamino)propyl)carbodiimide; EDTA, ethylenediaminetetraacetic acid; ELISA, enzyme-linked immunosorbent assay; Et, ethyl; HER2, human epidermal growth factor receptor 2; HIC, hydrophobic interaction chromatography; HMW, high molecular weight; HOBt, 1-hydroxybenzotriazole; HPLC, high-performance liquid chromatography; HRP, horseradish peroxidase; HSA, human serum albumin; LC, liquid chromatography; Me, methyl; MMAE, monomethylauristatin E; MOM, methoxymethyl; Ms, mesyl; MS, mass spectrometry; NBS, *N*-bromosuccinimide; PABA, *p*-aminobenzyl alcohol; PK, pharmacokinetics; *i*-Pr, isopropyl; SEC, size exclusion chromatography; SEM, standard error of the mean; TAb, total antibody; TCEP, tris(2-carboxyethyl)phosphine; THF, tetrahy-

DOI: 10.1021/mp500781a
Mol. Pharmaceutics 2015, 12, 1813−1835

drofuran; TFA, trifluoroacetic acid; TFAA, trifluoroacetic anhydride; Tmab, trastuzumab; TMB, 3,3′,5,5′-tetramethylbenzidine; UPLC, ultra performance liquid chromatography

REFERENCES

(1) Okeley, N. M.; Alley, S. C.; Senter, P. D. Advancing Antibody–Drug Conjugation. From the Laboratory to a Clinically Approved Anticancer Drug. *Hematol. Oncol. Clin. N. Am.* **2014**, *28*, 13–25.

(2) Lambert, J. M.; Chari, R. V. J. Ado-Trastuzumab Emtansine (T-DM1): An Antibody–Drug Conjugate (ADC) for HER2-Positive Breast Cancer. *J. Med. Chem.* **2014**, *58*, 6949–6964.

(3) Chari, R. V. J.; Miller, M. L.; Widdison, W. C. Antibody–Drug Conjugates: An Emerging Concept in Cancer Therapy. *Angew. Chem., Int. Ed.* **2014**, *53*, 3796–3827.

(4) Perez, H. L.; Cardarelli, P. M.; Deshpande, S.; Gangwar, S.; Schroeder, G. M.; Vite, G. D.; Borzilleri, R. M. Antibody–Drug Conjugates: Current Status and Future Directions. *Drug Discovery Today* **2014**, *19*, 869–881.

(5) Miller, M.; Fishkin, N.; Li, W.; Reid, E.; Archer, K.; Maloney, E.; Kovtun, Y.; Jones, G.; Ellis, M.; Singh, R.; Whiteman, K.; Pinkas, J.; Chari, R. New Class of DNA-Alkylating Agents with a Suitable Tolerability Profile Created for Use in Antibody–Drug Conjugates (ADCs). In *Proceedings of the AACR-NCI-EORTC International Conference: Molecular Targets and Cancer Therapeutics*, Boston, MA, October 19–23, 2013; AACR: Philadelphia, PA, 2013; Vol. *12* (11 Suppl), abstract no. C160.

(6) Gopal, A. K.; Ramchandren, R.; O'Conner, O. A.; Berryman, R. B.; Advani, R. H.; Chen, R.; Smith, S. E.; Cooper, M.; Rothe, A.; Matous, J. V.; Grove, L. E.; Zain, J. Safety and Efficacy of Brentuximab Vedotin for Hodgkin Lymphoma Recurring after Allogeneic Stem Cell Transplantation. *Blood* **2012**, *120*, 560–568.

(7) Younes, A.; Gopal, A. K.; Smith, S. E.; Ansell, S. M.; Rosenblatt, J. D.; Savage, K. J.; Ramchandren, R.; Bartlett, N. L.; Cheson, B. D.; de Vos, S.; Forero-Torres, A.; Moskowitz, C. H.; Connors, J. M.; Engert, A.; Larsen, E. K.; Kennedy, D. A.; Sievers, E. L.; Chen, R. Results of a Pivotal Phase II Study of Brentuximab Vedotin for Patients with Relapsed or Refractory Hodgkin's Lymphoma. *J. Clin. Oncol.* **2012**, *30*, 2183–2189.

(8) Pro, B.; Advani, R.; Brice, P.; Bartlett, N. L.; Rosenblatt, J. D.; Illidge, T.; Matous, J.; Ramchandren, R.; Fanale, M.; Connors, J. M.; Yang, Y.; Sievers, E. L.; Kennedy, D. A.; Shustov, A. Brentuximab-Vedotin (SGN-35) in Patients with Relapsed or Refractory Systemic Anaplastic Large-Cell Lymphoma: Results of a Phase II Study. *J. Clin. Oncol.* **2012**, *30*, 2190–2196.

(9) Burris, H. A., III; Rugo, H. S.; Vukelja, S. J.; Vogel, C. L.; Borson, R. A.; Limentani, S.; Tan-Chiu, E.; Krop, I. E.; Michaelson, R. A.; Girish, S.; Amler, L.; Zheng, M.; Chu, Y. W.; Klencke, B.; O'Shaughnessy, J. A. Phase II Study of the Antibody–Drug Conjugate Trastuzumab-DM1 for the Treatment of Human Epidermal Growth Factor Receptor 2 (HER2)-Positive Breast Cancer after Prior HER2-Directed Therapy. *J. Clin. Oncol.* **2011**, *29*, 398–405.

(10) Krop, I. E.; LoRusso, P.; Miller, K. D.; Modi, S.; Yardley, D.; Rodriguez, G.; Guardino, E.; Lu, M.; Zheng, M.; Girish, S.; Amler, L.; Winer, E. P.; Rugo, H. S. A Phase II Study of Trastuzumab Emtansine in Patients with Human Epidermal Growth Factor Receptor 2-Positive Metastatic Breast Cancer Who Were Previously Treated with Trastuzumab, Lapatinib, an Anthracycline, a Taxane, and Capecitabine. *J. Clin. Oncol.* **2012**, *30*, 3234–3241.

(11) Verma, S.; Miles, D.; Gianni, L.; Krop, I. E.; Welslau, M.; Baselga, J.; Pegram, M.; Oh, D. Y.; Dieras, V.; Guardino, E.; Fand, L.; Lu, M. W.; Olsen, S.; Blackwell, K. Trastuzumab Emtansine for HER2-Positive Advanced Breast Cancer. *N. Engl. J. Med.* **2012**, *367*, 1783–1791.

(12) Hurvitz, S. A.; Dirix, L.; Kocsis, J.; Bianchi, G. V.; Lu, J.; Vinholes, J.; Guardino, E.; Song, C.; Tong, B.; Ng, V.; Chu, Y. W.; Perez, E. A. Phase II Randomized Study of Trastuzumab Emtansine Versus Trastuzumab Plus Docetaxel in Patients with Human Epidermal Growth Factor Receptor 2-Positive Metastatic Breast Cancer. *J. Clin. Oncol.* **2013**, *31*, 1157–1163.

(13) Sassoon, I.; Blanc, V. Antibody–Drug Conjugate (ADC) Clinical Pipeline: A Review. In *Antibody–Drug Conjugates, Methods in Molecular Biology*; Ducry, L., Ed.; Humana Press: New York, 2013; Vol. *1045*, pp 1–27.

(14) Hanka, L. J.; Dietz, A.; Gerpheide, S. A.; Kuentzel, S. L.; Martin, D. G. CC-1065 (NSC-298223), a New Anti-Tumor Antibiotic. Production, in Vitro Biological Activity, Microbiological Assays and Taxonomy of the Producing Microorganism. *J. Antibiot.* **1978**, *31*, 1211–1217.

(15) Boger, D. L.; Johnson, D. S. CC-1065 and the Duocarmycins: Understanding Their Biological Function through Mechanistic Studies. *Angew. Chem., Int. Ed.* **1996**, *35*, 1438–1474.

(16) Martin, D. G.; Biles, C.; Gerpheide, S. H.; Hanka, L. J.; Krueger, W. C.; McGovren, J. P.; Mizsak, S. A.; Neil, G. L.; Stewart, J. C.; Visser, J. CC-1065 (NSC 298223), a Potent New Antitumor Agent. Improved Production and Isolation, Characterization and Antitumor Activity. *J. Antibiot.* **1981**, *34*, 1119–1125.

(17) McGovren, J. P.; Clarke, G. L.; Pratt, E. A.; DeKoning, T. F. Preliminary Toxicity Studies with the DNA-Binding Antibiotic, CC-1065. *J. Antibiot.* **1984**, *37*, 63–70.

(18) Boger, D. L. The Duocarmycins: Synthetic and Mechanistic Studies. *Acc. Chem. Res.* **1995**, *28*, 20–29.

(19) Boger, D. L.; Boyce, C. W.; Garbaccio, R. M.; Goldberg, J. A. CC-1065 and the Duocarmycins: Synthetic Studies. *Chem. Rev.* **1997**, *97*, 787–828.

(20) Cacciari, B.; Romagnoli, R.; Baraldi, P. G.; Da Ros, T.; Spalluto, G. CC-1065 and the Duocarmycins: Recent Developments. *Expert Opin. Ther. Pat.* **2000**, *10*, 1853–1871.

(21) Ghosh, N.; Sheldrake, H. M.; Searcey, M.; Pors, K. Chemical and Biological Explorations of the Family of CC-1065 and the Duocarmycin Natural Products. *Curr. Top. Med. Chem.* **2009**, *9*, 1494–1524.

(22) Boger, D. L.; Ishizaki, T.; Zarrinmayeh, H.; Munk, S. A.; Kitos, P. A.; Suntornwat, O. Duocarmycin–Pyrindamycin DNA Alkylation Properties and Identification, Synthesis, and Evaluation of Agents Incorporating the Pharmacophore of the Duocarmycin–Pyrindamycin Alkylation Subunit. Identification of the CC-1065-Duocarmycin Common Pharmacophore. *J. Am. Chem. Soc.* **1990**, *112*, 8961–8971.

(23) Jin, W.; Trzupek, J. D.; Rayl, T. J.; Broward, M. A.; Vielhauer, G. A.; Weir, S. J.; Hwang, I.; Boger, D. L. A Unique Class of Duocarmycin and CC-1065 Analogues Subject to Reductive Activation. *J. Am. Chem. Soc.* **2007**, *129*, 15391–15397.

(24) Cristofanilli, M.; Bryan, W. J.; Miller, L. L.; Chang, A. Y. C.; Gradishar, W. J.; Kufe, D. W.; Hortobagyi, G. N. Phase II Study of Adozelesin in Untreated Metastatic Breast Cancer. *Anti-Cancer Drugs* **1998**, *9*, 779–782.

(25) Pavlidis, N.; Aamdal, S.; Awada, A.; Calvert, H.; Fumoleau, P.; Sorio, R.; Punt, C.; Verweij, J.; van Oosterom, A.; Morant, R.; Wanders, J.; Hanauske, A. R. Carzelesin Phase II Study in Advanced Breast, Ovarian, Colorectal, Gastric, Head and Neck Cancer, Non-Hodgkin's Lymphoma and Malignant Melanoma: a Study of the EORTC Early Clinical Studies Group (ECSG). *Cancer Chemother. Pharmacol.* **2000**, *46*, 167–171.

(26) Markovic, S. N.; Suman, V. J.; Vukov, A. M.; Fitch, T. R.; Hillman, D. W.; Adjei, A. A.; Alberts, S. R.; Kaur, J. S.; Braich, T. A.; Leitch, J. M.; Creagan, E. T. Phase II Trial of KW2189 in Patients with Advanced Malignant Melanoma. *Am. J. Clin. Oncol.–Cancer Clin. Trials* **2002**, *25*, 308–312.

(27) Jeffrey, S. C.; Nguyen, M. T.; Moser, R. F.; Meyer, D. L.; Miyamoto, J. B.; Senter, P. D. Minor Groove Binder Antibody Conjugates Employing a Water Soluble β-Glucuronide Linker. *Bioorg. Med. Chem. Lett.* **2007**, *17*, 2278–2280.

(28) Jeffrey, S. C.; Torgov, M. Y.; Andreyka, J. B.; Boddington, L.; Cerveny, C. G.; Denny, W. A.; Gordon, K. A.; Gustin, D.; Haugen, J.; Kline, T.; Nguyen, M. T.; Senter, P. D. Design, Synthesis, and in Vitro Evaluation of Dipeptide-Based Antibody Minor Groove Binder Conjugates. *J. Med. Chem.* **2005**, *48*, 1344–1358.

DOI: 10.1021/mp500781a
Mol. Pharmaceutics 2015, 12, 1813–1835

(29) Chari, R. V. J.; Jackel, K. A.; Bourret, L. A.; Derr, S. M.; Tadayoni, B. M.; Mattocks, K. M.; Shah, S. A.; Liu, C. N.; Blattler, W. A.; Goldmacher, V. S. Enhancement of the Selectivity and Antitumor Efficacy of a CC-1065 Analog through Immunoconjugate Formation. *Cancer Res.* **1995**, *55*, 4079−4084.
(30) Zhao, R. Y.; Erickson, H. K.; Leece, B. A.; Reid, E. E.; Goldmacher, V. S.; Lambert, J. M.; Chari, R. V. J. Synthesis and Biological Evaluation of Antibody Conjugates of Phosphate Prodrugs of Cytotoxic DNA Alkylators for the Targeted Treatment of Cancer. *J. Med. Chem.* **2012**, *55*, 766−782.
(31) Bristol-Myers Squibb. Study of MDX-1203 in Subjects with Advanced/Recurrent Clear Cell Renal Cell Carcinoma (ccRCC) or Relapsed/Refractory B-Cell Non-Hodgkin's Lymphoma (B-NHL). http://clinicaltrials.gov/show/NCT00944905 (accessed Jan 12, 2015).
(32) Owonikoko, T. K.; Hussain, A.; Stadler, W. M.; Smith, D. C.; Sznol, M.; Molina, A. M.; Gulati, P.; Shah, A.; Ahlers, C. M.; Cardarelli, J.; Cohen, L. J. A Phase 1 Multicenter Open-Label Dose-Escalation Study of BMS-936561 (MDX-1203) in Clear Cell Renal Cell Carcinoma (ccRCC) and B-cell Non Hodgkin Lymphoma (B-NHL). In *Proceedings of the 2014 ASCO Annual Meeting*, Chicago, IL, May 30−June 3, 2014; ASCO: Alexandria, VA, 2014; Vol. *32* (15 Suppl), abstract no. 2558.
(33) Boger, D. L.; Ishizaki, T.; Wysocki, R. J., Jr.; Munk, S. A.; Kitos, P. A.; Suntornwat, O. Total Synthesis and Evaluation of (±)-*N*-(*tert*-Butoxycarbonyl)-CBI, (±)-CBI-CDPI1, and (±)-CBI-CDPI2: CC-1065 Functional Agents Incorporating the Equivalent 1,2,9,9a-Tetrahydrocyclopropa[1,2-*c*]benz[1,2-*e*]indol-4-one (CBI) Left-Hand Subunit. *J. Am. Chem. Soc.* **1989**, *111*, 6461−6463.
(34) Boger, D. L.; Munk, S. A. DNA Alkylation Properties of Enhanced Functional Analogs of CC-1065 Incorporating the 1,2,9,9a-Tetrahydrocyclopropa[1,2-*c*]benz[1,2-*e*]indol-4-one (CBI) Alkylation Subunit. *J. Am. Chem. Soc.* **1992**, *114*, 5487−5496.
(35) Stobbe, H. A New Synthesis of Tetraconic Acid. *Chem. Ber.* **1893**, *26*, 2312−2319.
(36) Kastrinsky, D. B.; Boger, D. L. Effective Asymmetric Synthesis of 1,2,9,9a-Tetrahydrocyclopropa[*c*]benzo[*e*]indol-4-one (CBI). *J. Org. Chem.* **2004**, *69*, 2284−2289.
(37) Boger, D. L.; McKie, J. A.; Boyce, C. W. Asymmetric Synthesis of the CBI Alkylation Subunit of the CC-1065 and Duocarmycin Analogs. *Synlett* **1997**, 515−517.
(38) Tichenor, M. S.; Trzupek, J. D.; Kastrinsky, D. B.; Shiga, F.; Hwang, I.; Boger, D. L. Asymmetric Total Synthesis of (+)- and Ent-(−)-Yatakemycin and Duocarmycin SA: Evaluation of Yatakemycin Key Partial Structures and Its Unnatural Enantiomer. *J. Am. Chem. Soc.* **2006**, *128*, 15683−15696.
(39) Tietze, L.; Schuster, H.; Hampel, S.; Rühl, S.; Pfoh, R. Enantio- and Diastereoselective Synthesis of Duocarmycine-Based Prodrugs for a Selective Treatment of Cancer by Epoxide Opening. *Chem.—Eur. J.* **2008**, *14*, 895−901.
(40) Tietze, L. F.; Behrendt, F.; Major, F.; Krewer, B.; von Hof, J. M. Synthesis of Fluorescence-Labelled Glycosidic Prodrugs Based on the Cytotoxic Antibiotic Duocarmycin. *Eur. J. Org. Chem.* **2010**, 6909−6921.
(41) Tschitschibabin, A. E. Tautomerie in der Pyridin-Reihe. *Ber. Dtsch. Chem. Ges.* **1927**, *60*, 1607−1617.
(42) Lee, J.; Kim, H. J.; Choi, S.; Choi, H. G.; Yoon, S.; Kim, J.-H.; Jo, K.; Kim, S.; Koo, S.-Y.; Kim, M.-H.; Kim, J. I.; Hong, S.-Y.; Kim, M. S.; Ahn, S.; Yoon, H.-S.; Cho, H. S. Novel 3-(2-Amino-4-pyrimidinyl)-4-hydroxyphenyl Ketone Derivatives. Int. Pat. Appl. WO 2004/080979.
(43) Dokter, W. H.; Ubink, R.; van der Lee, M.; van der Vleuten, M.; van Achterberg, T.; Jacobs, D.; Loosveld, E.; van den Dobbelsteen, D.; Egging, D.; Mattaar, E.; Groothuis, P.; Beusker, P.; Coumans, R.; Elgersma, R.; Menge, W.; Joosten, J.; Spijker, H.; Huijbregts, T.; de Groot, V.; Eppink, M.; de Roo, G.; Verheijden, G.; Timmers, M. Preclinical Profile of the HER2-Targeting ADC SYD983/SYD985; Introduction of a New Duocarmycin-Based Linker-Drug Platform. *Mol. Cancer Ther.* **2014**, *13*, 2618−2629.
(44) LogP values were calculated with ChemBioDraw Ultra (version 14.0.0.117) from PerkinElmer, Inc.
(45) Armarego, W. L. F. Ionization and Ultraviolet Spectra of Indolizines. *J. Chem. Soc.* **1964**, 4226−4233.
(46) Paudler, W. W.; Blewitt, H. L. Ten π Electron Nitrogen Heterocycle Compounds. V. The Site of Protonation and N-Methylation of Imidazo[1,2-*a*]pyridines and the Planarity of the Ring System. *J. Org. Chem.* **1966**, *31*, 1295−1298.
(47) Dubowchik, G. M.; Firestone, R. A. Cathepsin B-Sensitive Dipeptide Prodrugs. 1. A Model Study of Structural Requirements for Efficient Release of Doxorubicin. *Bioorg. Med. Chem. Lett.* **1998**, *8*, 3341−3346.
(48) de Groot, F. M. H.; Loos, W. J.; Koekkoek, R.; van Berkom, L. W. A.; Busscher, G. F.; Seelen, A. E.; Albrecht, C.; de Bruijn, P.; Scheeren, H. W. Elongated Multiple Electronic Cascade and Cyclization Spacer Systems in Activatible Anticancer Prodrugs for Enhanced Drug Release. *J. Org. Chem.* **2001**, *66*, 8815−8830.
(49) Amir, R. J.; Pessah, N.; Shamis, M.; Shabat, D. Self-Immolative Dendrimers. *Angew. Chem., Int. Ed.* **2003**, *42*, 4494−4499.
(50) Bouvier, E.; Thirot, S.; Schmidt, F.; Monneret, C. A New Paclitaxel Prodrug for Use in ADEPT Strategy. *Org. Biomol. Chem.* **2003**, *1*, 3343−3352.
(51) Kobayashi, E.; Okamoto, A.; Asada, M.; Okabe, M.; Nagamura, S.; Asai, A.; Saito, H.; Gomi, K.; Hirata, T. Characteristics of Antitumor Activity of KW-2189, a Novel Water-Soluble Derivative of Duocarmycin, against Murine and Human Tumors. *Cancer Res.* **1994**, *54*, 2404−2410.
(52) Derwin, D. W.; Passmore, D.; Zhang, Q.; Sufi, B.; Pan, C.; Rao, C.; Huber, M.; Gangwar, S.; Cardarelli, P.; Deshpande, S.; Rangan, V. Enzymology of the Mechanism of Action for MDX-1203 Antibody Drug Conjugate. In *Proceedings of the 103rd Annual Meeting of the American Association for Cancer Research*, Chicago, IL, March 31−April 4, 2012; AACR: Philadelphia, PA, 2012; Vol. *72* (8 Suppl), abstract no. LB-252.
(53) Dubowchik, G. M.; Firestone, R. A.; Padilla, L.; Willner, D.; Hofstead, S. J.; Mosure, K.; Knipe, J. O.; Lasch, S. J.; Trail, P. A. Cathepsin B-Labile Dipeptide Linkers for Lysosomal Release of Doxorubicin from Internalizing Immunoconjugates: Model Studies of Enzymatic Drug Release and Antigen-Specific in Vitro Anticancer Activity. *Bioconjugate Chem.* **2002**, *13*, 855−869.
(54) Beusker, P. H.; Coumans, R. G. E.; Elgersma R. C.; Menge, W. M. P. B.; Joosten, J. A. F.; Spijker, H. J.; de Groot, F. M. H. Novel Conjugates of CC-1065 Analogs and Bifunctional Linkers. Int. Patent Appl. WO 2011/133039.
(55) Dokter, W. H. A.; van der Lee, M. M. C.; Groothuis, P.; Ubink, R.; van der Vleuten, M. A. J.; van Achterberg, T. A.; Loosveld, E. M.; Damming, D.; Jacobs, D. C. H.; Rouwette, M.; Egging, D. F.; van den Dobbelsteen, D.; Beusker, P. H.; Goedings, P.; Verheijden, G. F. M.; Lemmens, J. M.; Timmers, M. The Preclinical Profile of the Duocarmycin-Based HER2-Targeting ADC SYD985 Predicts for Clinical Benefit in Low HER2-Expressing Breast Cancers. *Mol. Cancer. Ther.* **2015**, x DOI: 10.1158/1535-7163.MCT-14-0881-T.
(56) Hollander, I.; Kunz, A.; Hamann, P. Selection of Reaction Additives Used in the Preparation of Monomeric Antibody-Calicheamicin Conjugates. *Bioconjugate Chem.* **2007**, *19*, 358−361.
(57) Boger, D. L.; Garbaccio, R. M. Shape-Dependent Catalysis: Insights into the Source of Catalysis for the CC-1065 and Duocarmycin DNA Alkylation Reaction. *Acc. Chem. Res.* **1999**, *32*, 1043−1052.
(58) European Medicines Agency. EMA/702390/2012. Committee for Medicinal Products for Human Use: Assessment Report Adcetris. http://www.ema.europa.eu/docs/en_GB/document_library/EPAR_-_Public_assessment_report/human/002455/WC500135054.pdf (accessed Jan 12, 2015).
(59) Poon, K. A.; Flagella, K.; Beyer, J.; Tibbitts, J.; Kaur, S.; Saad, O.; Yi, J. H.; Girish, S.; Dybdal, N.; Reynolds, T. Preclinical Safety Profile of Trastuzumab Emtansine (T-DM1): Mechanism of Action of Its Cytotoxic Component Retained with Improved Tolerability. *Toxicol. Appl. Pharmacol.* **2013**, *273*, 298−313.

DOI: 10.1021/mp500781a
Mol. Pharmaceutics 2015, 12, 1813−1835

(60) Alley, S. C.; Benjamin, D. R.; Jeffrey, S. C.; Okeley, N. M.; Meyer, D. L.; Sanderson, R. J.; Senter, P. D. Contribution of Linker Stability to the Activities of Anticancer Immunoconjugates. *Bioconjugate Chem.* **2008**, *19*, 759−765.
(61) Shen, B. Q.; Xu, K.; Liu, L.; Raab, H.; Bhakta, S.; Kenrick, M.; Parsons-Reponte, K. L.; Tien, J.; Yu, S. F.; Mai, E.; Li, D.; Tibbitts, J.; Baudys, J.; Saad, O. M.; Scales, S. J.; McDonald, P. J.; Hass, P. E.; Eigenbrot, C.; Nguyen, T.; Solis, W. A.; Fuji, R. N.; Flagella, K. M.; Patel, D.; Spencer, S. D.; Khawli, L. A.; Ebens, A.; Wong, W. L.; Vandlen, R.; Kaur, S.; Sliwkowski, M. X.; Scheller, R. H.; Polakis, P.; Junutula, J. R. Conjugation Site Modulates the in Vivo Stability and Therapeutic Activity of Antibody−Drug Conjugates. *Nat. Biotechnol.* **2012**, *30*, 184−189.
(62) Hamblett, K. J.; Senter, P. D.; Chace, D. F.; Sun, M. M. C.; Lenox, J.; Cerveny, C. G.; Kissler, K. M.; Bernhardt, S. X.; Kopcha, A. K.; Zabinski, R. F.; Meyer, D. L.; Francisco, J. A. Effects of Drug Loading on the Antitumor Activity of a Monoclonal Antibody Drug Conjugate. *Clin. Cancer Res.* **2004**, *10*, 7063−7070.
(63) Lombardo, F.; Shalaeva, M. Y.; Tupper, K. A.; Gao, F. ElogDoct: A Tool for Lipophilicity Determination in Drug Discovery. 2. Basic and Neutral Compounds. *J. Med. Chem.* **2001**, *44*, 2490−2497.
(64) Kerns, E. H.; Di, L.; Petusky, S.; Kleintop, T.; Huryn, D.; McConnell, O.; Carter, G. Pharmaceutical Profiling Method for Lipophilicity and Integrity Using Liquid Chromatography−Mass Spectrometry. *J. Chromatogr. B* **2003**, *791*, 381−388.

DOI: 10.1021/mp500781a
Mol. Pharmaceutics 2015, 12, 1813−1835